The Plastidic Sugar Transporter pSuT Influences Flowering and Affects Cold Responses[1[OPEN]]

Kathrin Patzke,[a,2] Pratiwi Prananingrum,[a,2] Patrick A.W. Klemens,[a] Oliver Trentmann,[a] Cristina Martins Rodrigues,[a] Isabel Keller,[a] Alisdair R. Fernie,[b] Peter Geigenberger,[c] Bettina Bölter,[c] Martin Lehmann,[c] Stephan Schmitz-Esser,[d] Benjamin Pommerrenig,[a] Ilka Haferkamp,[a] and H. Ekkehard Neuhaus[a,3,4]

[a]Plant Physiology, University of Kaiserslautern, D-67653 Kaiserslautern, Germany
[b]Max Planck Institut for Molecular Plant Physiology, Wissenschaftspark Golm, D-14476 Potsdam, Germany
[c]Ludwig Maximilians University Munich, Biocenter, Department II, D-82152 Planegg-Martinsried, Germany
[d]Department of Animal Science, Iowa State University, Ames, Iowa 50011-3150

ORCID IDs: 0000-0001-7380-0779 (K.P.); 0000-0002-4849-1537 (C.M.R.); 0000-0001-9000-335X (A.R.F.); 0000-0001-9512-349X (P.G.); 0000-0002-7780-7289 (B.B.); 0000-0002-7522-7942 (B.P.); 0000-0002-7432-3190 (I.H.); 0000-0002-5443-7123 (H.E.N.).

Sucrose (Suc) is one of the most important types of sugars in plants, serving inter alia as a long-distance transport molecule, a carbon and energy storage compound, an osmotically active solute, and fuel for many anabolic reactions. Suc biosynthesis and degradation pathways are well known; however, the regulation of Suc intracellular distribution is poorly understood. In particular, the cellular function of chloroplast Suc reserves and the transporters involved in accumulating these substantial Suc levels remain uncharacterized. Here, we characterize the plastidic sugar transporter (pSuT) in Arabidopsis (*Arabidopsis thaliana*), which belongs to a subfamily of the monosaccharide transporter-like family. Transport analyses with yeast cells expressing a truncated, vacuole-targeted version of pSuT indicate that both glucose and Suc act as substrates, and nonaqueous fractionation supports a role for pSuT in Suc export from the chloroplast. The latter process is required for a correct transition from vegetative to reproductive growth and influences inflorescence architecture. Moreover, pSuT activity affects freezing-induced electrolyte release. These data further underline the central function of the chloroplast for plant development and the modulation of stress tolerance.

Biological membranes separate cells from the external environment and separate individual intracellular compartments from each other. Thus, to fulfill their physiological functions, biological membranes must exhibit a certain degree of impermeability but also guarantee the controlled passage of a plethora of solutes, including metabolites, ions, gases, and signal molecules. The abundance and composition of channel and transport proteins, their activities, substrate specificities, and modes of transport determine the specific solute permeability of individual biological membranes.

Among the metabolites transported across plant cell membranes, sugars are of particular physiological relevance, as they act as fuel for energy metabolism and provide precursors in many anabolic reactions. In addition to this, sugars influence the onset of flowering, govern fruit quality and organ architecture, and contribute to biotic and abiotic stress tolerance (Hoekstra et al., 2001; Hanson and Smeekens, 2009; Weichert et al., 2010; Bolouri Moghaddam and Van den Ende, 2013; Sun et al., 2014; Chen et al., 2015b; Naseem et al., 2017; Pommerrenig et al., 2018).

Since sugars affect a wide range of cell and organ responses, tight control of their intercellular and intracellular distribution is mandatory. The distribution of sugars is regulated by specific sugar transport proteins found in the plasma membrane and in membranes of various organelles (Bush, 1999; Martinoia et al., 2007; Chen et al., 2015a; Hedrich et al., 2015). For example, the transport of monosaccharides or disaccharides across the plasma membrane plays an important role in long-distance carbohydrate partitioning between source and sink tissues, whereas vacuolar sugar transport has great impact on intracellular sugar levels and composition (Hedrich et al., 2015). In the plasma membrane or the vacuolar membrane (tonoplast), several sugar transporters have been identified at the molecular level, and their characterization provided important insights into their protein structures, transport modes, and

[1]This work was supported by the Deutsche Forschungsgemeinschaft (TRR 175 The Green Hub-Central Coordinator of Acclimation in Plants).

[2]These authors contributed equally to the article.

[3]Author for contact: neuhaus@rhrk.uni-kl.de.

[4]Senior author

The author responsible for distribution of materials integral to the findings presented in this article in accordance with the policy described in the Instructions for Authors (www.plantphysiol.org) is: Ekkehard Neuhaus (neuhaus@rhrk.uni-kl.de).

K.P., P.P., P.A.W.K., B.B., C.M.R., I.K., M.L., O.T., P.G., and A.R.F. conducted experiments and analyzed samples; S.S.-E. performed phylogenetic analyses; B.P., I.H., and H.E.N. wrote the article; O.T., I.H., and H.E.N. developed conceptual strategies; O.T. and H.E.N. led the project.

[OPEN]Articles can be viewed without a subscription.

www.plantphysiol.org/cgi/doi/10.1104/pp.18.01036

regulation of transport activities as well as their physiological functions (Chen et al., 2015b; Hedrich et al., 2015; Tao et al., 2015; Julius et al., 2017).

Chloroplasts also are able to transport sugars across their membranes. However, although the protein-mediated import of sugars into the chloroplast has been known for decades (Wang and Nobel, 1971; Schäfer and Heber, 1977), so far only two plastidic sugar transporters have been identified at the molecular level. These transporters reside in the inner envelope membrane of the chloroplast and either mediate the export of maltose (Maltose Exporter1 [MEX1]; Niittylä et al., 2004; Findinier et al., 2017) or catalyze glucose (Glc) translocation (Plastidic Glc Transporter [pGlcT]; Weber et al., 2000). In *mex1* loss-of-function mutants, the defective maltose export results in stromal maltose accumulation that markedly inhibits starch degradation and causes pronounced growth retardation (Niittylä et al., 2004; Lu and Sharkey, 2006), whereas Arabidopsis (*Arabidopsis thaliana*) mutants lacking pGlcT do not differ substantially from wild-type plants (Cho et al., 2011). Interestingly, in addition to maltose and Glc, which represent sugars derived from starch degradation, chloroplasts also contain raffinose and Suc in their stroma. However, the synthesis of these sugars occurs exclusively in the cytosol; thus, specific transport proteins for these sugars were postulated to reside in the chloroplast envelope (Schneider and Keller, 2009; Nägele and Heyer, 2013).

In contrast to MEX1, the transporter pGlcT is a member of the large monosaccharide transporter-like (MST) family. In Arabidopsis, the MST family comprises 53 members (Büttner, 2007; Johnson and Thomas, 2007; Pommerrenig et al., 2018), and detailed phylogenetic analyses showed that transporters with related biochemical properties cluster together, thus forming seven functional MST subfamilies. Some of these subfamilies contain many transporter isoforms, such as the SUGAR TRANSPORTER PROTEIN or the EARLY RESPONSE TO DEHYDRATION-like group, whereas the two groups TONOPLAST SUGAR TRANSPORTER (TST) and VACUOLAR GLUCOSE TANSPORTER (VGT) represent the smallest subfamilies, each with only three isoforms (Büttner, 2007; Johnson and Thomas, 2007; Pommerrenig et al., 2018).

From these three VGT isoforms, solely VGT1 has been functionally characterized in more detail and identified to act as a proton-coupled sugar antiporter, catalyzing Glc uptake into the vacuole (Aluri and Büttner, 2007). VGT1 function is required for proper seed germination and flower development, possibly by modulating cell turgor (Aluri and Büttner, 2007). Even though the biochemical function of VGT2 is not known, its high structural similarity to VGT1 suggests that it also resides in the tonoplast and acts as a Glc/H^+ antiporter (Aluri and Büttner, 2007). In a recent chloroplast-targeting approach, the leader sequence of the third VGT isoform, previously named HP59 protein (a predicted D-Xyl transporter; Hector et al., 2008), was identified to be sufficient for the targeting of cyanobacterial transporters to chloroplasts (Rolland et al., 2016). The apparent chloroplast location of HP59 suggests that this protein functions as a plastidic sugar transporter, although this has not been demonstrated yet.

In this study, we performed a comprehensive characterization of HP59, here named Plastidic Sugar Transporter (pSuT) due to its intracellular localization, biochemical properties, and physiological impact. By employing heterologous expression of pSuT in yeast, we demonstrate that this plastid-localized VGT homolog in fact mediates proton-driven Glc allocation, similar to VGT1. Unexpectedly, we also identified the disaccharide Suc as an additional substrate of pSuT. By studying *pSuT* T-DNA insertion lines with reduced transport activity, we gained valuable insights into its physiological role. The results obtained suggest that the mobilization of plastidic Suc reserves is a factor important for plant developmental processes, like the initiation of flowering or the determination of inflorescence architecture. Moreover, pSuT-mediated Suc export out of chloroplasts modulates abiotic stress tolerance in Arabidopsis, as demonstrated by the impaired response of mutants to cold temperatures.

RESULTS

pSuT Contains Internal Domains Typical for Sugar Transport Proteins and Exhibits an N-Terminal Extension

The Arabidopsis MST family comprises more than 50 proven or predicted monosaccharide transporters, organized in seven individual clusters (Büttner, 2007; Pommerrenig et al., 2018; Supplemental Fig. S1). Functional characterization of diverse MST family members led to the finding that the phylogenetic relation reflects a functional relation, since proteins with identical or at least similar properties cluster together. Consequently, phylogenetic subclusters represent functional subfamilies. The candidate plastidic sugar transporter pSuT belongs to the VGT subfamily. VGT1 and VGT2 represent close homologs, whereas pSuT is more distantly related to these transporters (Supplemental Fig. S1).

An alignment of their amino acid sequences provided insights into similarities and differences between VGT1, VGT2, and pSuT (Supplemental Fig. S2). Similar to other sugar transporters of prokaryotes and eukaryotes (Saier, 2000), all members of the VGT subfamily exhibit 12 predicted transmembrane domains (TM) and a comparatively large, centrally located hydrophilic loop, which is about 75 amino acid residues in length and connects TMs 6 and 7. The assumption that pSuT functions as a sugar carrier is strongly supported by the presence of four conserved amino acid sequences, namely DxxGRR between TMs 2/3 and TMs 8/9, PASPRWL between TMs 6/7, and PETKG C terminal to TM 12 (Supplemental Fig. S2, red boxes). All of these motifs are highly conserved among sugar transporters of prokaryotic and eukaryotic cells (Henderson, 1991).

All VGT subfamily members share a high number of conserved amino acid residues. However, VGT1 and VGT2 exhibit higher similarities to each other (89%

sequence similarity) than to pSuT (VGT1, 69%; VGT2, 70%). It becomes immediately evident that the N terminus of pSuT differs markedly from that of the remaining VGTs, particularly due to its extension by 50 amino acids (Supplemental Fig. S2). Moreover, pSuT possesses a sequence section in the centrally located hydrophilic loop that also differs from the remaining two VGTs.

Targeting Analysis with pSuT and pSuT Hybrid Proteins

Closer inspection of the N terminus of pSuT led to the finding that it contains a nonproportionally high number of Ser residues, a characteristic often observed for protein precursors targeted to the chloroplast. Moreover, it is composed of a chloroplast transit peptide (Supplemental Fig. S2; first 31 amino acids, shaded in green) and the so-called membrane protein leader (sequence between the chloroplast transit peptide and the first TM). This kind of bipartite targeting sequence is a typical feature of multipass inner envelope membrane proteins with 10 or more TMs (Rolland et al., 2016). Therefore, the amino acid sequence analysis already points to a plastidic localization, which was verified experimentally by analyses of pSuT-GFP fusions. Transient expression of pSuT in tobacco (*Nicotiana tabacum*) or Arabidopsis mesophyll protoplasts resulted in a GFP signal that encloses the autofluorescence of the chloroplasts (Fig. 1A; Rolland et al., 2016).

To confirm that the N-terminal domain of pSuT contains a classical transit peptide, which is removed after translocation, a protein import assay was conducted. To this end, we generated a [^{35}S]Met-labeled pSuT precursor by in vitro translation and incubated isolated pea (*Pisum sativum*) chloroplasts with this preparation. Note that, for unknown reasons, the in vitro translation efficiency of the full-length pSuT precursor was extremely low. Thus, we expressed a C-terminally truncated version of the pSuT precursor, lacking the last six predicted TMs (prepSuT-6TM). The corresponding radioactively labeled translation product appeared at the expected molecular mass of about 36 kD (Supplemental Fig. S3, left). After incubation of

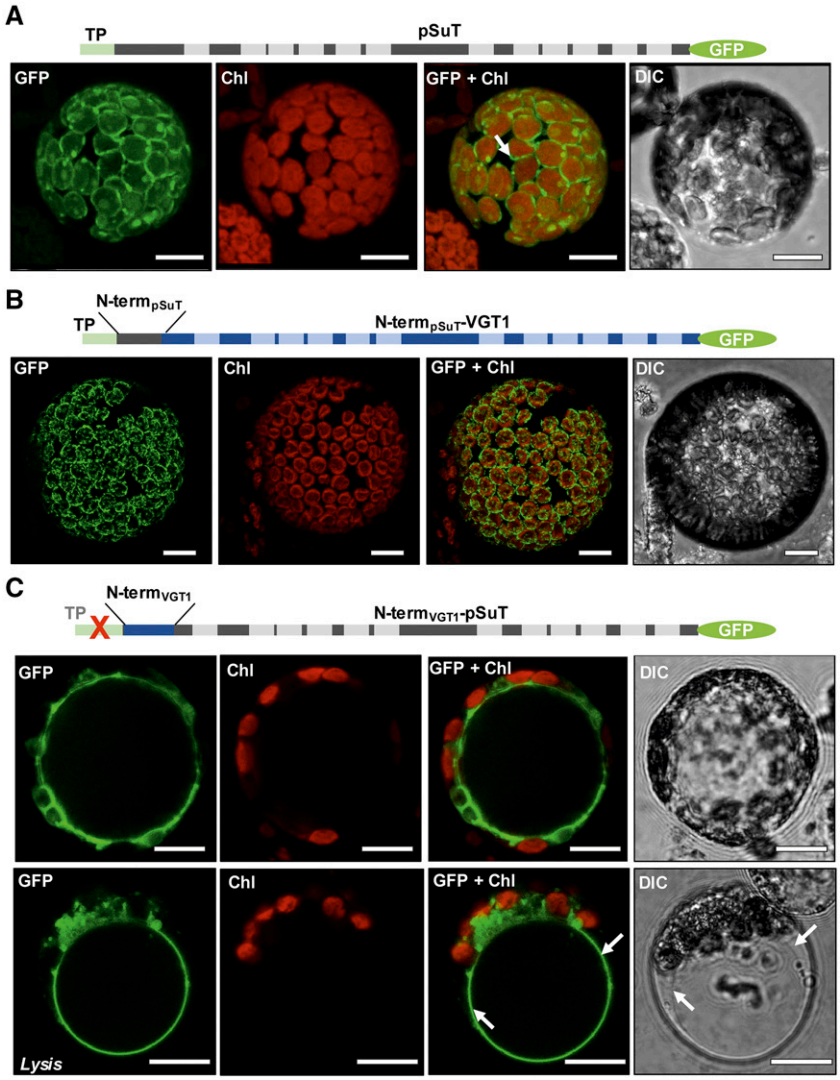

Figure 1. Subcellular localization of pSuT-GFP and pSuT hybrid-GFP fusions. Confocal images show transiently transformed Arabidopsis mesophyll protoplasts. From left to right: GFP fluorescence (GFP), chlorophyll autofluorescence (Chl), fluorescence overlay (GFP + Chl), and Nomarski differential interference contrast (DIC). Schematic illustrations of the fusion constructs are shown above the microscopic images. A, Transient expression of pSuT-GFP carrying the native pSuT N terminus with the chloroplast transit peptide (TP) in maximum projection. GFP fluorescence is confined to the plastid envelope membrane (arrow). B, Transient expression of VGT1-GFP with the VGT1 N terminus replaced by the N terminus of pSuT including the chloroplast transit peptide (N-term$_{pSuT}$-VGT1) in maximum projection. GFP fluorescence is confined to the plastid envelope. C, Transient expression of pSUT-GFP with the pSuT N terminus replaced by the N terminus of VGT1 (N-term$_{VGT1}$-pSuT) and without the pSuT chloroplast transit peptide in optical sections. Tonoplast targeting of GFP by N-term$_{VGT1}$-pSuT is supported by gentle lysis of the protoplast and release of the vacuole (Lysis). Arrows indicate the positions of the tonoplast. Bars = 10 μm.

pea chloroplasts with prepSuT-6TM, two protein bands became detectable (Supplemental Fig. S3, middle). The top band exhibits a molecular mass identical to that of the translation product, whereas the bottom band appeared at an apparent molecular mass of about 30 kD. Incubation of the chloroplast with thermolysin revealed that the larger protein is susceptible to this protease and, thus, represents the plastid-attached, but nonimported, prepSuT-6TM. The smaller protein is resistant to thermolysin cleavage. Therefore, we can conclude that the mature protein is incorporated into the plastid envelope and that a domain of an apparent molecular mass of 6 kD is removed from prepSuT-6TM by stromal signal peptidases. In this context, it is necessary to mention that the chloroplast transit peptide possesses a smaller predicted molecular mass (~3.6 kD). Without specific experimental approaches, it is not possible to identify why the apparent molecular mass of the mature protein is lower than predicted. It might result from (1) the removal of an N-terminal fragment larger than the predicted transit peptide, (2) increased total hydrophobicity (and thus underestimated size of the mature protein), or (3) limitations in precise molecular mass determination on the basis of the autoradiogram.

Interestingly, the bipartite N termini of different multipass inner envelope membrane proteins (including pSuT) were shown recently to be capable of directing ectopically expressed cyanobacterial bicarbonate transporters to plant chloroplasts, whereas the corresponding chloroplast transit peptides were not sufficient (Rolland et al., 2016). To analyze whether it is possible to exploit the bipartite N-terminal targeting sequence of pSuT for the redirection of a vacuolar transporter to the chloroplast and whether N-terminal domain swapping even allows the redirection of pSuT to the vacuole, we created corresponding hybrid constructs. For this, we replaced the first 38 amino acid residues of VGT1-GFP with the N terminus of pSuT, or we replaced the first 89 amino acid residues of pSuT-GFP with the N terminus of VGT1 (Supplemental Fig. S2, blue triangle). The resulting GFP fusion constructs were termed N-termpSuT-VGT1 and N-termVGT1-pSuT, respectively.

Transient expression of N-termpSuT-VGT1 in isolated Arabidopsis protoplasts revealed a plastidic localization of this fusion protein, since the GFP signal surrounds the autofluorescence of the chloroplasts (Fig. 1B). This GFP pattern is highly similar to that of the pSuT-GFP fusion protein (Fig. 1A). Therefore, we conclude that VGT1 was not only directed to the chloroplast by the N terminus of pSuT but finally also becomes inserted into the envelope membrane. Interestingly, a similar result was obtained when the bipartite N-terminal domain of pSuT was fused to SUC4, a vacuolar sugar transporter of a different protein family (Supplemental Fig. S4A).

By contrast, the N-termVGT1-pSuT fusion protein does not locate to chloroplasts but apparently accumulates in the vacuolar membrane (Fig. 1C). This conclusion is based on the following findings. First, the GFP signal does not overlap with the plasma membrane. Second, it labels a large and space-filling organelle partly indented by several red-fluorescing chloroplasts. Finally, it persists after gentle protoplast lysis and release of the vacuole. This pattern is identical to that caused by the VGT1-GFP fusion protein (Supplemental Fig. S4B) and other vacuolar sugar transporters (Wormit et al., 2006; Jung et al., 2015).

VGT1 and pSuT Differ in Terms of Their Substrate Spectra

Characteristics of its amino acid sequence (12 TMs, the long central loop between TMs 6 and 7, and the four sugar-binding motifs; Supplemental Fig. S2) already classify pSuT as a sugar transporter. Moreover, the close relationship (Supplemental Fig. S1) and high sequence similarity (Supplemental Fig. S2) to VGT1 (Aluri and Büttner, 2007) suggest that pSuT also acts as a Glc/proton antiporter. However, experimental evidence for this function was so far lacking. To this end, we studied the sugar transport activity of pSuT by heterologously expressing the ΔTP-pSuT gene (lacking the chloroplast transit peptide) in baker's yeast (*Saccharomyces cerevisiae*). This truncated pSuT-GFP fusion protein localized to the yeast vacuole (Supplemental Fig. S5). To this end, we used the yeast strain W303, which is unaltered in sugar transport and catabolizing processes compared with the wild type and, therefore, possesses the complete genetic repertoire coding for monosaccharide transporters (Bisson et al., 1993).

First, we analyzed the ability of yeast cells harboring either a vector carrying a ΔTP-pSuT-GFP expression cassette or an empty control vector to grow on Glc medium with or without 0.2% (w/v) 2-deoxyglucose (2-dGlc; Fig. 2). 2-dGlc is a Glc derivative transportable by Glc carriers; it is generally toxic to cells but becomes detoxified by its sequestration into the vacuole (Weiss and Hiltbrand, 1985). Therefore, growth analyses with 2-dGlc allow for the identification of a possible Glc transport activity of transporters. Both control cells and ΔTP-pSuT-GFP-transformed cells exhibited similar growth on agar medium containing Glc (Fig. 2A). However, the growth of control yeast cells on agar medium containing Glc plus 2-dGlc was inhibited more severely when compared with the growth of ΔTP-pSuT-GFP-expressing cells (Fig. 2B). To produce quantitative data, we recorded substrate-dependent growth curves of both control and ΔTP-pSuT-GFP-transformed yeast cells in a plate reader. In the presence of solely Glc, both control cells and ΔTP-pSuT-GFP-harboring cells again exhibited nearly identical growth characteristics (Fig. 2C), whereas the additional presence of 2-dGlc significantly reduced the growth of control cells when compared with that of the ΔTP-pSuT-GFP-harboring cells (Fig. 2D). After 60 h, the optical density of the control was about 64% lower than that of the ΔTP-pSuT-GFP-transformed yeast cells (set to 100%).

The 2-dGlc transport data indicate that ΔTP-pSuT-GFP mediates the efficient sequestration of toxic 2-dGlc into the vacuole, which results in a growth advantage compared with that of the control (Fig. 2). Therefore, we can conclude that pSuT exhibits 2-dGlc and, likewise,

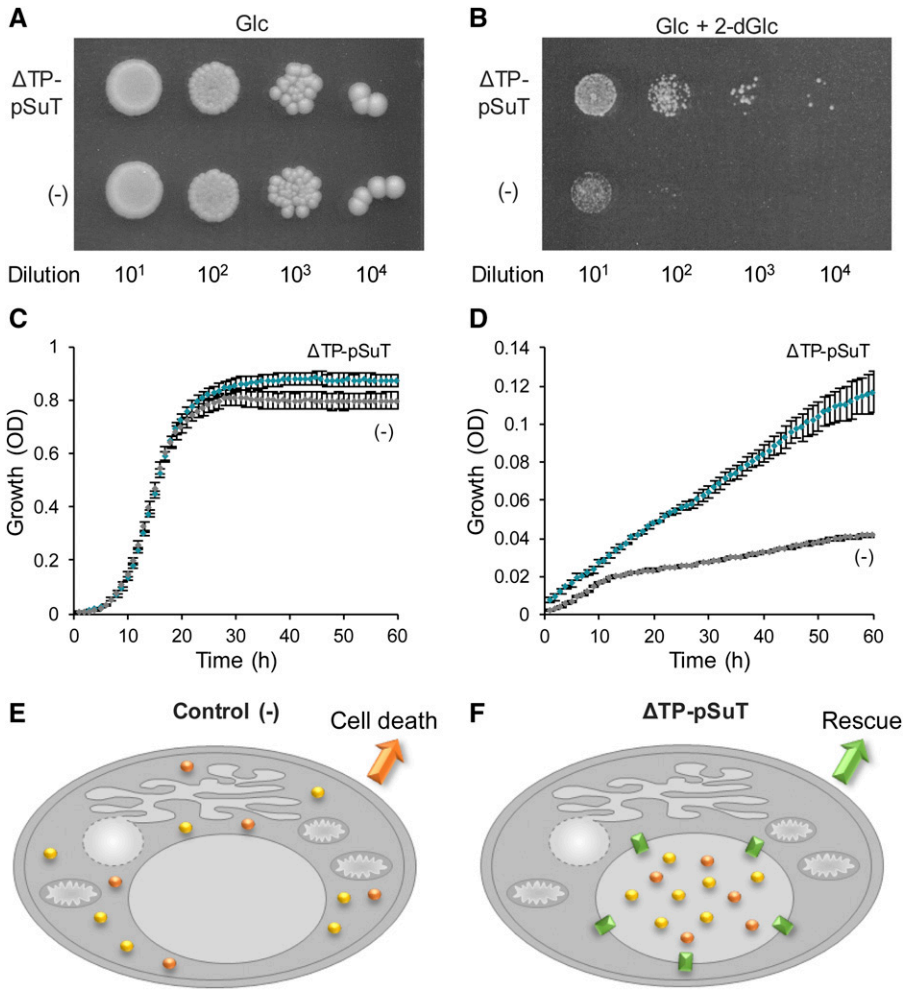

Figure 2. Growth of yeast W303 cells with 2-dGlc. A and B, Droplet test with yeast cells harboring the empty control vector (−) or the construct expressing a vacuole-targeted pSuT-GFP fusion (Supplemental Fig. S5) lacking its chloroplast transit peptide (ΔTP-pSuT). Cells were grown to an OD_{600} of 1, and serial dilutions were spotted on synthetic complete (SC) agar with 1% (w/v) Glc (A) or 1% (w/v) Glc plus 0.2% (w/v) 2-dGlc (B). C and D, Growth of yeast cells expressing ΔTP-pSuT in liquid SC medium with 2% (w/v) Glc (C) or 2% (w/v) Glc plus 0.2% (w/v) 2-dGlc (D). Data represent means of three independent biological replicates and at least three technical replicates ± SD. E and F, Schematic of the principle of the Glc 2-dGlc uptake assays. The pSuT-dependent sequestration into vacuoles results in the partial detoxification of 2-dGlc. Yellow spheres represent Glc, orange spheres represent 2-dGlc molecules, and green rectangles represent the GFP fusion of ΔTP-pSuT.

Glc transport activity. Moreover, because of the acidic pH of vacuoles, it is possible that Glc uptake via ΔTP-pSuT is driven by the antiport of protons.

To verify the Glc transport activity of ΔTP-pSuT (not fused to GFP) in the yeast vacuole by an alternative assay, we used microscopy to analyze the accumulation of fluorescent Glc analogs. Transport studies with the Glc and Suc analogs 2-(*N*-(7-nitrobenz-2-oxa-1,3-diazol-4-yl) amino)-2-deoxyglucose (2-NBDG) and esculin have been applied successfully for the characterization of Arabidopsis sugar transporters expressed in yeast (Gora et al., 2012; Nieberl et al., 2017; Rottmann et al., 2018b). In the heterologous host, however, the corresponding transporters located to the plasma membrane. Moreover, so far, it has not been demonstrated whether fluorescing sugar analogs also allow for the identification of the sugar transport activity of Arabidopsis carriers residing, after recombinant synthesis, in the yeast vacuole. To check for possible vacuolar Glc uptake, we incubated yeast control cells or ΔTP-pSuT-expressing cells in medium supplemented with 2-NBDG and monitored the subcellular distribution of its green fluorescence. Control cells accumulated 2-NBGD in the cytosol but not in a large space-filling zone of the cell, which represents the vacuole (Fig. 3A). This fluorescence pattern is in agreement with previous analyses of 2-NBGD uptake in yeast (Roy et al., 2015), indicating that yeast usually lacks the capacity to import Glc into the vacuole. In contrast, ΔTP-pSuT-expressing cells did not show high fluorescence in the cytosol but instead accumulated 2-NBGD in the vacuole (Fig. 3B).

The obtained data in sum suggest that pSuT, just like VGT1, acts as an H^+/Glc antiporter. Since VGT1 is incapable of transporting Suc (Aluri and Büttner, 2007), we hypothesized that pSuT also rejects this disaccharide. In order to investigate the transport specificity of pSuT, we analyzed the possible vacuolar uptake of esculin by the ΔTP-pSuT-expressing cells. However, yeast cells generally are incapable of Suc uptake from the medium. Therefore, to analyze possible vacuolar Suc uptake by pSuT, we first had to establish a Suc uptake system in the plasma membrane allowing for Suc import into the cell. To this end, we transformed control and ΔTP-pSuT-expressing yeast cells with an expression vector containing the coding sequence for the H^+/Suc symporter SUC2 from Arabidopsis and subsequently measured esculin uptake. In fact, control cells expressing AtSUC2 showed the accumulation of esculin, as indicated by blue

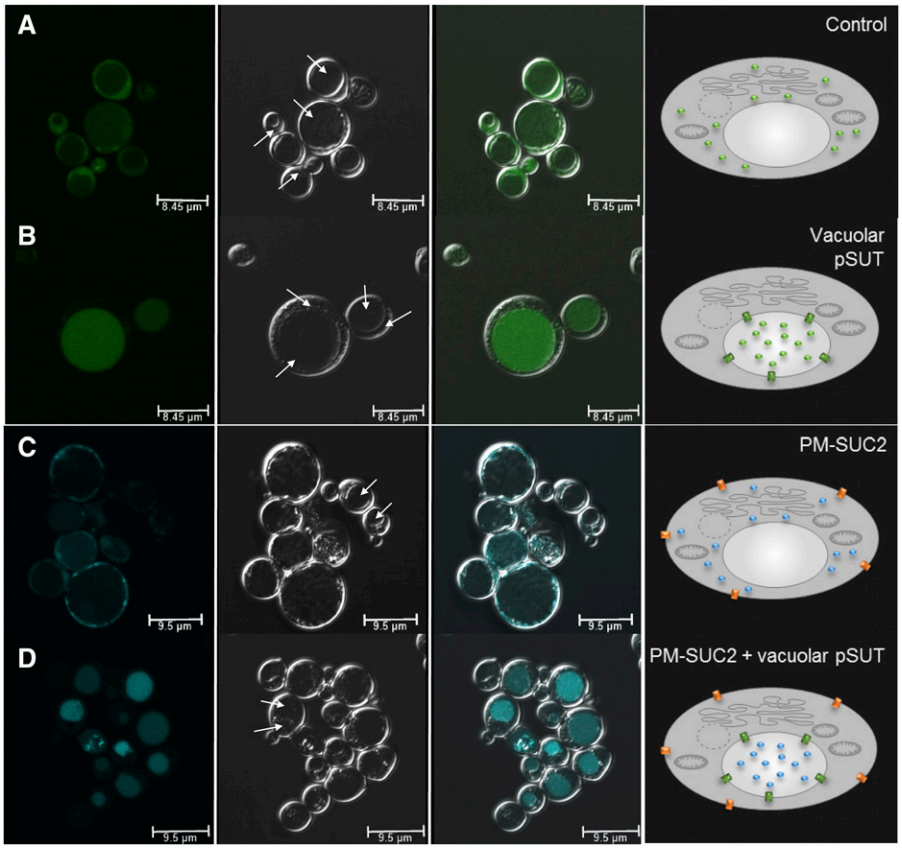

Figure 3. Uptake of fluorescent sugar derivatives. 2-NBDG and esculin uptake by yeast W303 cells is shown. The first image in each row (left) shows substrate-dependent fluorescence channels (494–551 nm for 2-NBDG and 465–600 nm for esculin). The second image shows the dark-field image, the third image shows the overlay, and the fourth image (right) shows a schematic representation of the underlying transport processes. Solid arrows point to the luminal side of vacuoles, and dashed arrows point to the cytosol. In the schemes, green spheres represent 2-NDBG, blue spheres represent esculin, green rectangles represent ΔTP-pSuT, and orange rectangles represent SUC2. A, 2-NBDG uptake into cells carrying a control vector. The green 2-NBDG-dependent fluorescence fills a broad zone within the cytosol. B, 2-NBDG uptake into cells carrying an expression vector with ΔTP-pSuT. The green 2-NBDG-dependent fluorescence is concentrated in vacuoles. C, Esculin uptake into cells expressing the plasma membrane Suc transporter SUC2 (PM-SUC2). The cyan esculin-dependent fluorescence fills a broad zone within the cytosol. D, Esculin uptake into cells carrying an expression vector with SUC2 (PM-SUC2) plus an expression vector with ΔTP-pSuT. The cyan esculin-dependent fluorescence is concentrated in vacuoles. Bars = 8.45 μm in A and B and 9.5 μm in C and D.

fluorescence, in the cytosol but not in the vacuole (Fig. 3C). In yeast cells harboring both AtSUC2 in the plasma membrane and ΔTP-pSuT in the vacuole, the blue fluorescence accumulated in their vacuoles (Fig. 3D). This result was unexpected and suggests that, besides Glc, pSuT is capable of transporting Suc against a concentration gradient across the vacuolar membrane (Fig. 3B).

We note that not all yeast cells exhibited similar vacuolar fluorescence. This observation probably is caused by the cell cycle phase-dependent activity of the promotor (*PMA1*) controlling the expression of *ΔTP-pSuT* (Supplemental Fig. S5; Nieberl et al., 2017).

pSuT Expression Is Detectable in Several Tissues and Repressed by Sugars

To gain insight into the developmental and tissue-specific expression of the *pSuT* gene in planta, we analyzed the activity of the *pSuT* promoter using a reporter-aided approach. To that end, we fused a 1,779-bp fragment upstream of the start codon of the *pSuT* gene to the reporter gene *uidA*, encoding the GUS reporter enzyme, and introduced the fusion construct into Arabidopsis. Transgenic plant lines were subjected to histochemical staining for GUS activity. The blue color is indicative of measurable *pSuT* promoter activity and was detectable in germinating seeds (Fig. 4), cotyledons of young seedlings (Fig. 4), the leaf meristem (Fig. 4E), photosynthetically active source leaves (Fig. 4F), and the peduncle and receptacle at the base of flower buds (Fig. 4G). In flowers, measurable amounts of GUS are present in young sepals, the style and ovary of the pistil, and the filament of the stamen (Fig. 4). Accordingly, the *pSuT* gene is apparently expressed in various young and mature tissues of vegetative to reproductive stages. The root generally exhibits rather low *pSuT* promoter activity.

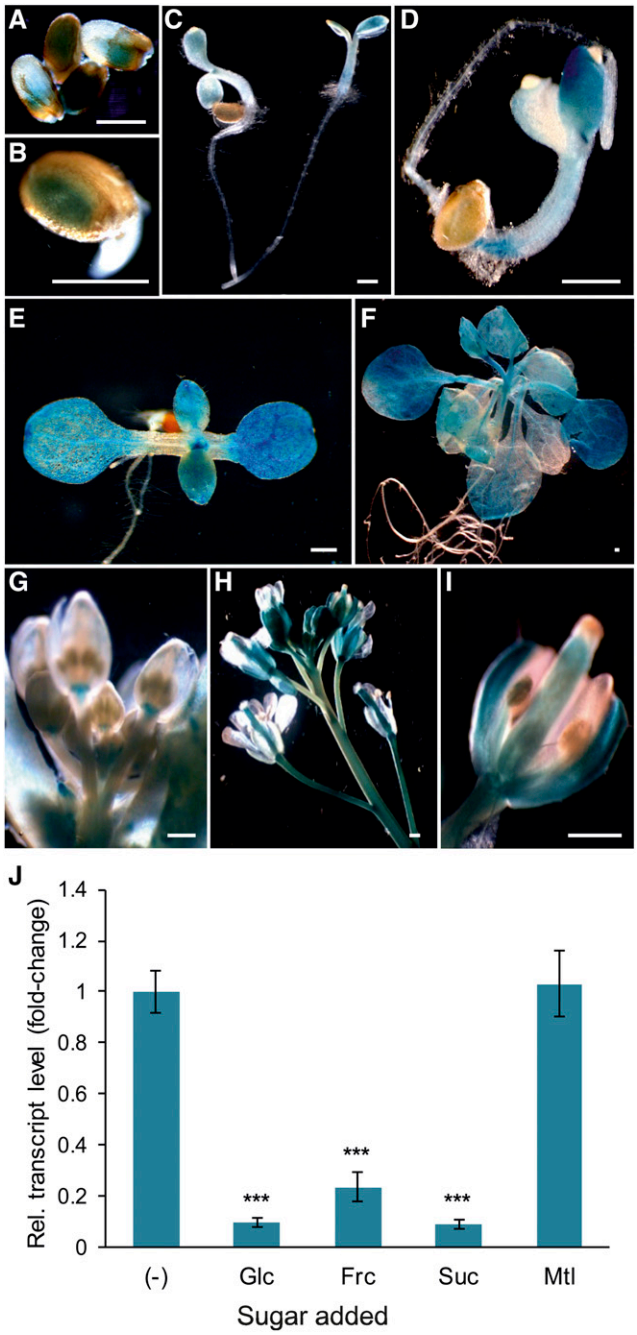

Figure 4. Analysis of the tissue-specific and sugar-dependent expression of *pSuT*. A to I, Transgenic plant lines expressing the glucoronidase reporter gene *uidA* under the control of the *pSuT* promoter were subjected to histochemical staining for GUS activity. A and B, GUS staining of germinating seeds. C and D, GUS staining in young seedlings. E, GUS staining in the cotyledons and the vegetative leaves of a 7-d-old seedling. F, GUS staining in rosette leaves of a 3-week-old plant. G, GUS staining of flower buds. H, GUS staining of an inflorescence. I, GUS staining of an opened flower. Bars = 0.5 mm. J, Expression of *pSuT* is repressed by exogenously supplied sugars. Leaf discs of 6-week-old wild-type plants were incubated in 300 mM Glc, Fru (Frc), Suc, mannitol (Mtl), or solely MES buffer as a reference (−). The data were normalized to the housekeeping genes *At4g26410*, *At1g13320*, and *At4g05320*. Fold change in expression was calculated relative to *pSuT* expression in MES buffer (set to 1). Data represent means of six biological replicates ± SE. Significant differences by one-tailed Student's *t* test (***, $P \leq 0.001$) are shown in relation to that in the reference sample (−).

It is well known that many genes encoding plant sugar transporters are responsive to changing cellular sugar levels (Wormit et al., 2006; Wingenter et al., 2010; Chardon et al., 2013; Klemens et al., 2013). To analyze possible sugar effects on *pSuT* expression, we incubated Arabidopsis leaf discs in buffer medium supplemented with different sugars and quantified the corresponding mRNA levels via reverse transcription quantitative PCR (RT-qPCR). The finding that the *pSuT* promoter exhibits moderate activity in rosette leaves under standard conditions (Fig. 4F) allows for the detection of a possible sugar-dependent enhanced or reduced *pSuT* expression in leaf discs. The presence of Glc, fructose (Fru), or Suc resulted in substantially lower *pSuT* mRNA accumulation (8%–22%) when compared with that in the control (MES buffer, set to 100%; Fig. 4J). Since the incubation of leaf discs in mannitol did not markedly change the *pSuT* mRNA level (103%), osmotic effects were not causative for the sugar-induced transcript reduction.

Isolation of pSuT Knockout and Knockdown Mutant Plants

To reveal the role of pSuT in carbohydrate metabolism and sugar-dependent processes, we recruited two independent T-DNA insertion lines with reduced *pSuT* mRNA levels. At first glance, the two mutant lines had a wild-type phenotype. The Salk_021796 line carries a T-DNA insertion in the second intron of the *pSuT* gene (Supplemental Fig. S6). Since RT-qPCR analyses revealed an almost complete absence of *pSuT* mRNA in this line (less than 2% of the wild-type level), it is considered a *pSuT* knockout mutant (*pSuT-ko*; Supplemental Fig. S6C). In the Sail_335_F05 line, the T-DNA insertion is located in the 5′ untranslated region of the *pSuT* gene (Supplemental Fig. S6). It exhibits about 24% of the *pSuT* transcript when compared with the wild type and, thus, represents a *pSuT* knockdown mutant (*pSuT-kd*; Supplemental Fig. S6C). In *pSuT-kd*, the T-DNA also is present in the 5′ untranslated region of the gene *At5g59240* on the opposite DNA strand. A corresponding RT-qPCR analysis indicated that the T-DNA insertion has no negative (but rather a positive) impact on *At5g59240* transcription (Supplemental Fig. S6D).

pSuT Mutants Exhibit Altered Suc Compartmentation

The finding that pSuT is a functional Glc and Suc transporter (Figs. 2 and 3) prompted us to check whether *pSuT* mutants exhibit altered sugar contents. After 7 h of light, when carbohydrate levels are generally high, Glc, Fru, and Suc levels of leaf tissues from the two *pSuT* mutant lines did not differ significantly from those of the wild type. The concentrations of Glc and

Suc were quite similar and ranged from 1.8 to 2 μmol g^{-1} fresh weight in the individual plant lines (Fig. 5A). The concentration of Fru was comparatively low and ranged from 0.2 μmol g^{-1} fresh weight in wild-type and *pSuT-kd* plants to about 0.3 μmol g^{-1} fresh weight in the *pSuT-ko* line. Similar to the sugar levels, the starch contents also were not altered substantially in *pSuT* mutant plants (Fig. 5B).

The total cellular amount of tested carbohydrates apparently remained unchanged by impaired pSuT activity. However, because of its localization in the plastid envelope (Fig. 1; Supplemental Fig. S3), we hypothesized that its absence might affect intracellular sugar distribution. The so-called nonaqueous fractionation (NAF) is a remarkably laborious method, but so far it represents the only experimental approach suited to determine metabolite levels in different compartments simultaneously (Krüger et al., 2011). We harvested leaf material of 4-week-old wild-type and *pSuT-ko* plants and fractionated the subcellular compartments via NAF. This analysis revealed similar subcellular distributions of Glc in wild-type and *pSuT-ko* plants. The cytosol and the vacuole each contained approximately half of the cellular Glc, whereas this sugar was almost absent in chloroplasts (Fig. 6A). We note that *pSuT-ko* plants showed slightly higher cytosolic (58%) and lower vacuolar (40%) Glc levels than wild-type plants. Moreover, impaired pSuT activity did not cause significant changes in the subcellular distribution of Fru. In wild-type and *pSuT-ko* plants, 15% and 28% of the total cellular Fru was found in chloroplasts, about 67% and 48% accumulated in the cytosol, and approximately 18% and 25% were present in the vacuole, respectively (Fig. 6B). However, the plastidic and cytosolic Suc compartmentation differed significantly between wild-type and *pSuT-ko* plants. Chloroplasts of *pSuT-ko* plants contained twice as much of the total cellular Suc (33%) than wild-type chloroplasts (16%; Fig. 6C). The plastidic Suc accumulation goes along with a significantly reduced cytosolic Suc level in *pSuT-ko* plants (52%) when compared with that of the wild type (76%). The vacuolar percentage rate of total cellular Suc was slightly but not significantly lower in wild-type plants (7%) than in *pSuT-ko* plants (15%; Fig. 6C). These data suggest that impaired pSuT function does not cause substantial changes in the total cellular concentration of the tested carbohydrates or in the compartmentation of Glc and Fru but, apparently, affects Suc delivery from the plastid to the cytosol.

We hypothesized that the altered Suc compartmentation in *pSuT* mutants might affect the expression of genes coding for Suc-converting enzymes. Interestingly, the expression of *VACUOLAR INVERTASE1* (*VI1*) was down-regulated not only by high Glc but also by elevated Suc levels (Supplemental Fig. S7A). Consequently, one might expect that wild-type leaves contain less *VI1* mRNA than those of the *pSuT* mutants. In fact, *pSuT* mutants exhibited approximately 2-fold more *VI1* transcript in their leaves than the wild type.

pSuT Mutants Are Impaired in Inflorescence Development

Suc and Glc not only represent metabolites but also are signaling compounds. Accordingly, alterations in the availability and distribution of these sugars may influence plant growth, development, and physiology (Wind et al., 2010). Moreover, Suc is a well-known factor controlling the transition to flowering (Corbesier et al., 1998; Roldán et al., 1999; Ohto et al., 2001).

At first glance, the two *pSuT* mutant lines have a wild-type phenotype when cultivated under short-day conditions. To check for possible differences in flowering transition, we transferred 4-week-old wild-type and *pSuT* mutant plants from short-day to long-day (LD) conditions and monitored early inflorescence development (Fig. 7A). Plants with shoots longer than 1 cm were defined as bolted. Fourteen days after transfer to LD, wild-type plants started bolting (10%), whereas all *pSuT* mutant plants persisted in the juvenile phase. Twenty-four hours later, more than 60% of the wild-type plants and about 20% of the *pSuT-kd* plants exhibited small shoots. By the following day, almost all wild-type plants, more than half of the *pSuT-kd* mutants, and about 7% of the *pSuT-ko* mutants had developed inflorescences. It took a further 24 and 48 h until all *pSuT-kd* and 93% of the *pSuT-ko* plants could be

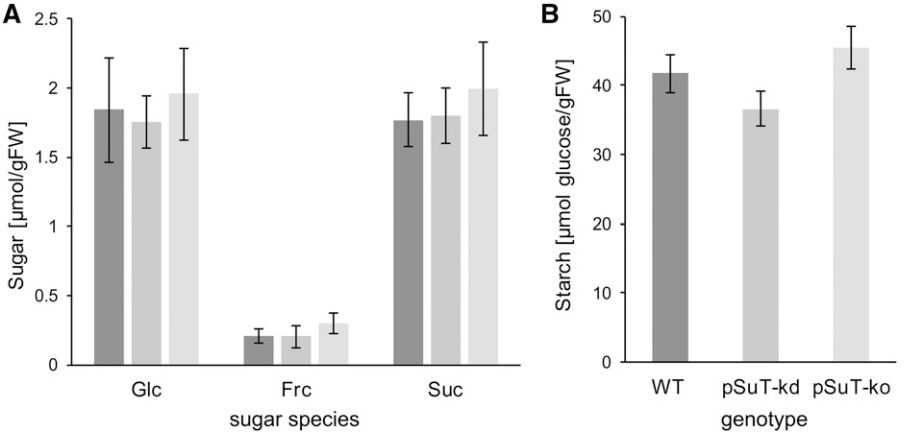

Figure 5. Carbohydrate levels of *pSuT* mutant plants. Reduced *pSuT* expression does not affect total cellular sugar and starch levels of leaves. Wild-type (WT) and *pSuT* mutant plants were cultivated under standard conditions (120 μE, 10 h of light/14 h of dark). Rosette leaves from 5-week-old plants were harvested at the end of the light phase (about 8 h in light). Carbohydrate levels were determined in leaf tissues from wild-type (dark gray bars), *pSuT-kd* (gray bars), and *pSuT-ko* (light gray bars) plants. A, Total cellular Glc, Fru (Frc), and Suc levels. B, Total cellular starch content. Data represent means of at least 14 biological replicates ± SE. FW, Fresh weight.

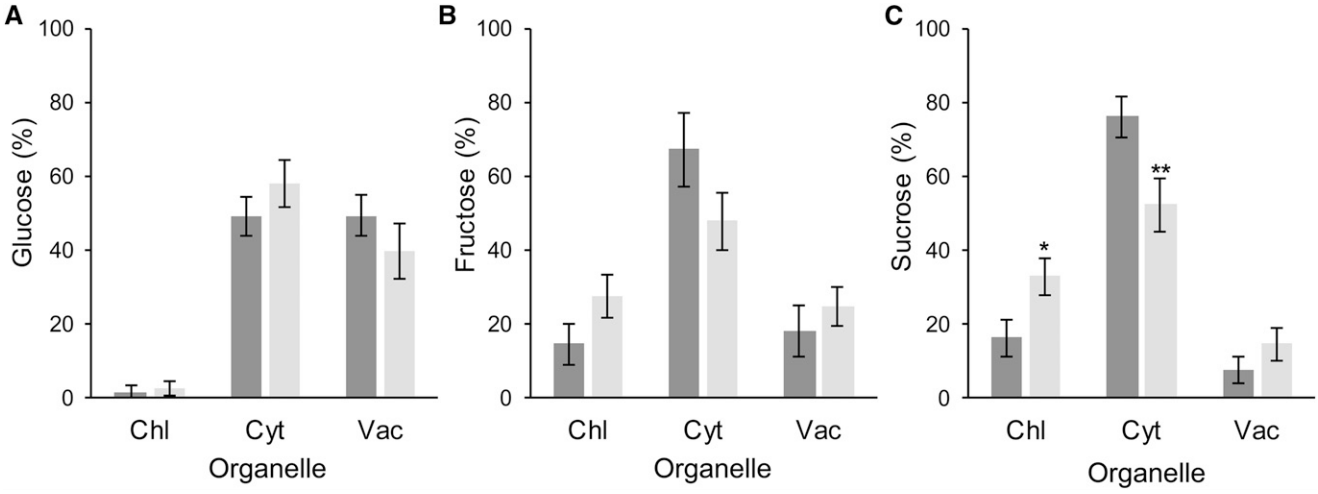

Figure 6. Analysis of subcellular sugars after NAF. Reduced *pSuT* expression affects subcellular sugar distribution. Leaf tissues of 4-week-old wild-type (dark gray bars) and *pSuT-ko* (light gray bars) plants were subjected to NAF. The distribution of Glc (A), Fru (B), and Suc (C) to chloroplasts (Chl), the cytosol (Cyt), and vacuoles (Vac) is shown. Data are means of nine biological replicates ± SE. Significant differences were calculated using one-tailed Student's *t* test (*, $P \leq 0.05$ and **, $P \leq 0.01$).

defined as bolted. Therefore, we conclude that the transition to flowering is delayed significantly in *pSuT-kd* and *pSuT-ko* plants.

Suc signaling, via trehalose-6-phosphate, is proposed to induce flowering by acting directly at the shoot apical meristem and by influencing FLOWERING LOCUS T (FT) signaling (Wahl et al., 2013). FT is a phloem-mobile protein interacting as a master regulator with transcription factors required for flowering initiation (Corbesier et al., 2007). Via RT-qPCR, we demonstrated that the relative expression of the *FT* gene is substantially lower in *pSuT-kd* and *pSuT-ko* plants when compared with corresponding *FT* mRNA levels in the wild type. The wild-type leaves contained more than twice as much *FT* mRNA as that present in the two *pSuT* mutant lines (Fig. 7B).

To check for further developmental differences between wild-type and *pSuT* mutant plants, we monitored inflorescence growth over time. Determination of the mean shoot length reflected the delay in bolting during the initial phase of flowering. However, it became apparent that the ongoing development of *pSuT* mutants also is retarded slightly when compared with that of the wild type (Fig. 7, C and D). For example, wild-type plants reached a mean stem length of 39.2 cm on day 31 in LD, and it took about 3 to 4 d longer until *pSuT-kd* and *pSuT-ko* plants approached this value (Fig. 7D). Similarly, the mean stem length of the *pSuT* mutants did not reach the wild-type level (at day 34 in LD), even if we consider their respective delays in flowering initiation (length at day 35 in LD for *pSuT-kd* and at day 36 in LD for *pSuT-ko*; Fig. 7D). These observations suggest that pSuT activity affects not only the onset of flowering but also the later reproductive phase.

To verify the possible impairment in the later reproductive phase and to correct for the observed delayed bolting onset, we harvested siliques from *pSuT-kd* and *pSuT-ko* plants 1 and 2 d later than those of the wild type. This analysis revealed that the *pSuT* mutant plants produce siliques that are reduced slightly in weight and length when compared with wild-type siliques (Fig. 8, A and B). In this context, it is important to mention that the reduced weight of the *pSuT* mutant siliques is most likely not caused by a generally lower weight of their seeds (Fig. 8C) but rather by the reduced number of seeds per silique (Fig. 8D). These results imply that pSuT activity is important during the initial as well as the later reproductive phases.

Interestingly, increasing data suggest that Suc mobility in plants, and its availability in buds, triggers bud outgrowth (Mason et al., 2014; Barbier et al., 2015; Otori et al., 2017). Besides its function as a valuable carbon source for general plant growth, Suc was shown to represent the first signal in the release of bud dormancy and, thus, represents a key component for the systemic regulation of shoot branching. Consequently, the lower cytosolic Suc level in *pSuT* mutants might extend bud dormancy in general. In fact, *pSuT* mutants appeared to have fewer inflorescence branches than the wild type (Fig. 9A). To examine quantitative data on bud outgrowth, we counted the number of primary rosette branches per plant. Wild-type plants exhibited 12 branches per plant on average, whereas the *pSuT* mutants produced about six branches per plant on average (Fig. 9B). These observations indicate that the impaired pSuT activity affects bud outgrowth and, thus, inflorescence architecture.

pSuT Mutants Exhibit Impaired Freezing Tolerance

Sugars represent the vast majority of compatible solutes, and their accumulation is not only one of the best-known responses to cold but also a basic mechanism in the acquisition of freezing tolerance (Levitt,

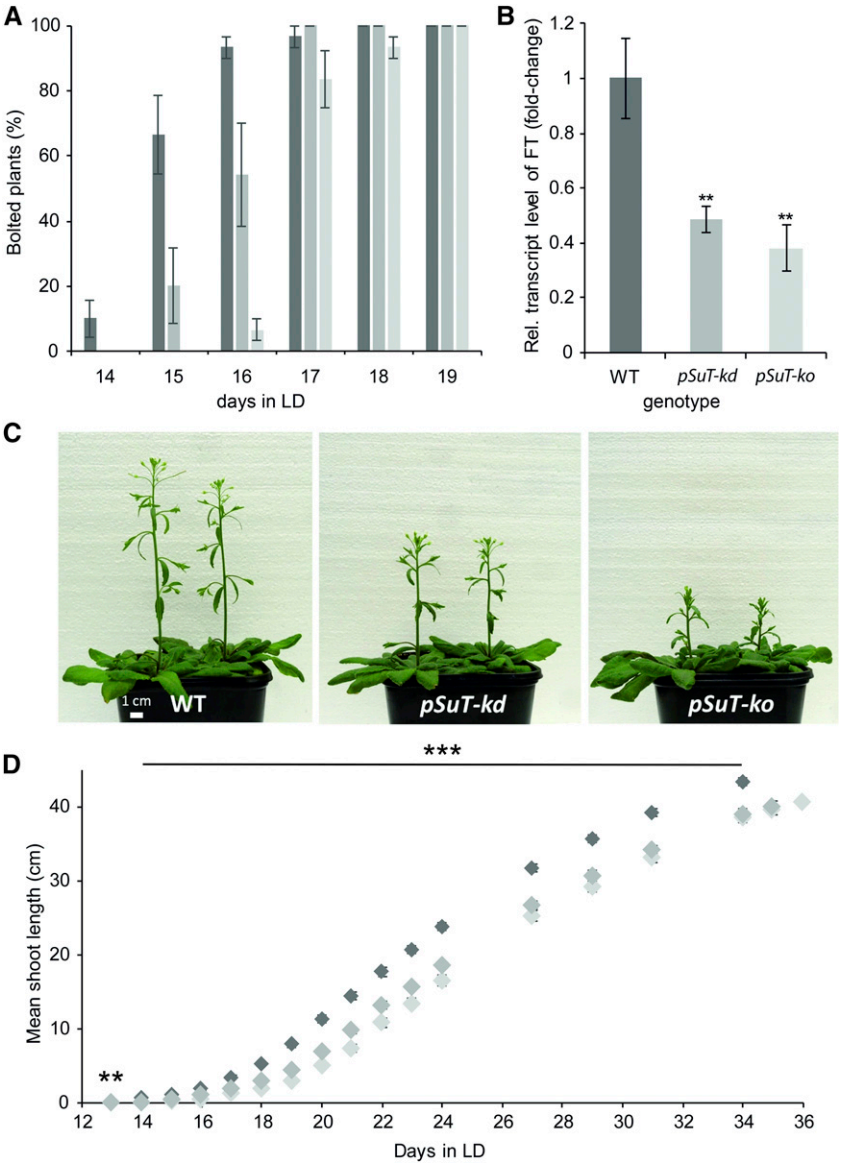

Figure 7. Analysis of the inflorescence development of wild-type (WT) and *pSuT* mutant plants. A, Determination of differences at the onset of bolting. Wild-type (dark gray bars), *pSuT-kd* (gray bars), and *pSuT-ko* (light gray bars) plants were cultivated for 4 weeks under standard conditions (120 μE, 10 h of light/14 h of dark) and transferred to LD conditions (250 μE, 16 h of light/8 h of dark) for flowering induction. When its shoot length reached 1 cm, the corresponding plant was defined as bolted. Data represent means ± SE of three replicates with nine or more plants each and are given as percentages of the total number of plants per genotype (set to 100%). B, Plants were cultivated as described in A. Youngest leaves covering the apical meristem were harvested shortly before bolting of the first wild-type plant (when its meristem leaves tended to erect). The relative transcript level of *FT* in the different genotypes is shown. *FT* expression in wild-type plants served as a reference (set to 1). Data were normalized to the housekeeping genes *At2g28390* and *At5g62690*. Data represent means of four or more biological replicates ± SE. Significant differences compared with the wild type were calculated using one-tailed Student's *t* test (**, $P \leq 0.01$). C, Representative wild-type, *pSuT-kd*, and *pSuT-ko* plants 20 d after their transfer to LD. D, Determination of the total shoot length of wild-type (dark gray diamonds), *pSuT-kd* (gray diamonds), and *pSuT-ko* (light gray diamonds) plants after transfer to LD. Data represent means ± SE of 29 or more individual plants per line. Significant differences compared with the wild type were calculated using one-tailed Student's *t* test (**, $P \leq 0.01$ and ***, $P \leq 0.001$).

1958; Alberdi and Corcuera, 1991; Nägele and Heyer, 2013; Pommerrenig et al., 2018). In this context, Suc plays a pivotal role. First, Suc can decrease membrane permeability by interacting directly with phospholipids of cell membranes (Strauss and Hauser, 1986). Second, carbon metabolism shifts from starch to Suc synthesis when plants grow in the cold (Strand et al., 1997, 1999). Third, the stimulation of Suc synthesis in mutant plants results in increased cold tolerance compared with the wild type (Strand et al., 2003). Fourth, Suc may become cleaved by invertases and, thus, increase the pool of Glc and Fru. Moreover, it may serve as a substrate for the synthesis of raffinose, an important cryoprotectant of chloroplasts, particularly of the photosystems (Knaupp et al., 2011).

Specific changes in sugar homeostasis and the subcellular distribution of the different sugars may allow for an adequate response to cold (Tarkowski and Van den Ende, 2015). Similarly, the expression levels and activities of vacuolar sugar transport proteins are influenced by cold temperatures and play a role in the acquisition of freezing tolerance (Wormit et al., 2006; Klemens et al., 2013, 2014; Guo et al., 2014; Le Hir et al., 2015). Because of its apparent Glc and Suc export capacity (Figs. 2 and 3), we hypothesized that pSuT also may be involved in the adaptation of the sugar compartmentation to cold. Therefore, we first analyzed whether cold temperatures cause alterations in *pSuT* mRNA levels. Twenty-four hours after the transfer of plants to 4°C, the expression of *pSuT* did not differ significantly from that of control plants kept at 22°C (Fig. 10A). However, we have to keep in mind that sugars accumulate strongly in response to cold temperatures and that *pSuT* expression becomes repressed by high sugar levels (Fig. 4B). Therefore, the sugar repression may conceal a possible cold-induced

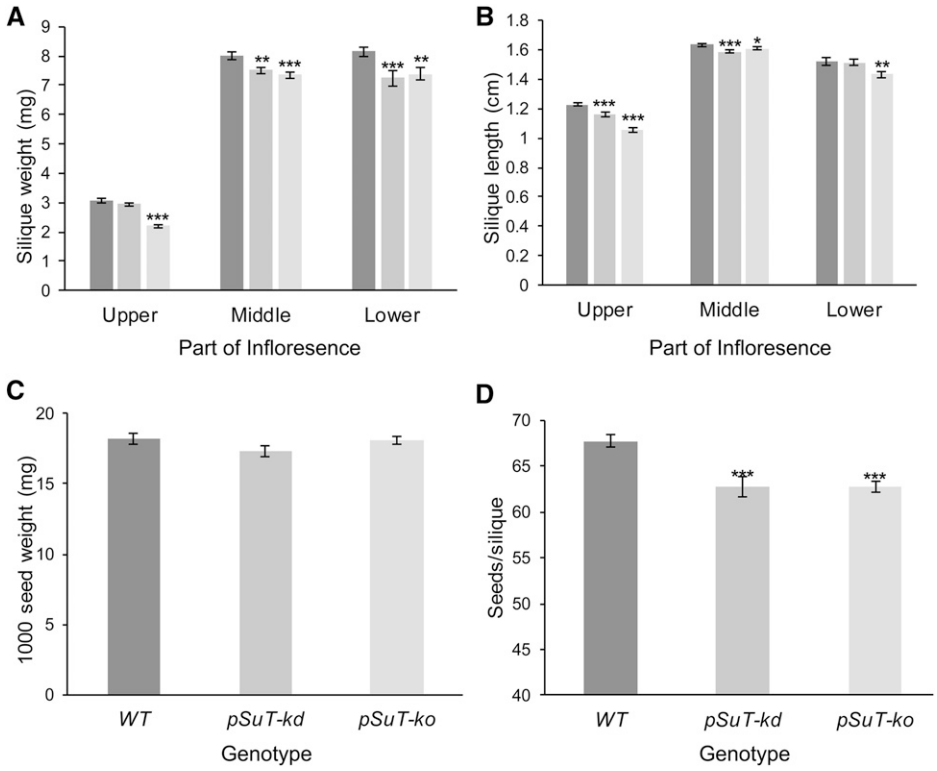

Figure 8. Analysis of siliques from wild-type (WT), *pSuT-kd*, and *pSuT-ko* plants. A and B, Analyses discriminated between young siliques (top part of the shoot), middle-aged siliques (middle part), and mature siliques (bottom part). For silique weight (A) and length (B) determination, five siliques of 29 or more plants were analyzed. Because of delayed bolting, *pSuT-kd* was analyzed 1 d and *pSuT-ko* was analyzed 2 d later than the wild type. C, Quantification of 1,000 seed weight was performed with 10 samples of seeds from two independent pools of at least 20 plants. D, Determination of the seed number per silique was performed with 70 or more siliques from five individual plants. Data represent means ± SE. Significant differences compared with the wild type were calculated using one-tailed Student's *t* test (*, $P \leq 0.05$; **, $P \leq 0.01$; and ***, $P \leq 0.001$).

stimulation of *pSuT* transcription. It has been shown that the rate and magnitude of sugar accumulation during cold acclimation essentially rely on photosynthetic activity (Wanner and Junttila, 1999). Consequently, we conducted cold treatment in the absence of light (24 h) to prevent the sugar repression of *pSuT* expression. Control plants also were transferred to darkness but, however, maintained at warm temperatures. The corresponding RT-qPCR analysis identified about 3-fold higher *pSuT* mRNA levels in these cold-treated plants when compared with those in the corresponding control (Fig. 10B). From these data, we conclude that the cold-induced stimulation counteracts sugar repression and helps to maintain *pSuT* expression even during cold temperatures.

Analyses of the subcellular distribution of sugars imply that chloroplasts can harbor a certain level of the total cellular Suc (16% [Fig. 6] or 30% [Fürtauer et al., 2016]). Therefore, these organelles might represent a possible reservoir for the fast provision of Suc via pSuT during cold temperatures. To gain insights into a possible role of pSuT in cold-dependent carbohydrate metabolism, we determined the sugar contents of leaves from *pSuT* mutant and wild-type plants exposed for 24 h to 4°C (Fig. 10C). No substantial alterations in Suc levels were detectable. However, leaves of *pSuT-kd* and *pSuT-ko* mutants show significantly lower Fru and particularly Glc levels than those of the wild type. The leaves of *pSuT* mutants contained around 14 μmol g^{-1} fresh weight Glc and about 8 to 8.5 μmol g^{-1} fresh

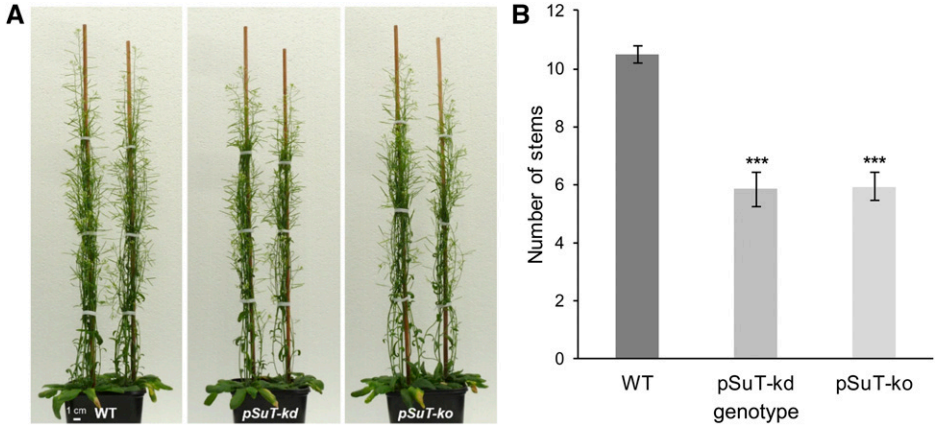

Figure 9. *pSuT* mutant plants exhibit fewer inflorescence stems than the wild type (WT). A, Representative images of 8-week-old wild-type, *pSuT-kd*, and *pSuT-ko* plants. B, Number of stems at the end of flowering. Because of the delay in bolting, *pSuT-kd* was analyzed 1 d and *pSuT-ko* was analyzed 2 d later than the wild type (34 d after transfer to LD). Data represent means ± SE of 29 or more individual plants per line. Significant differences compared with the wild type were calculated using one-tailed Student's *t* test (***, $P \leq 0.001$).

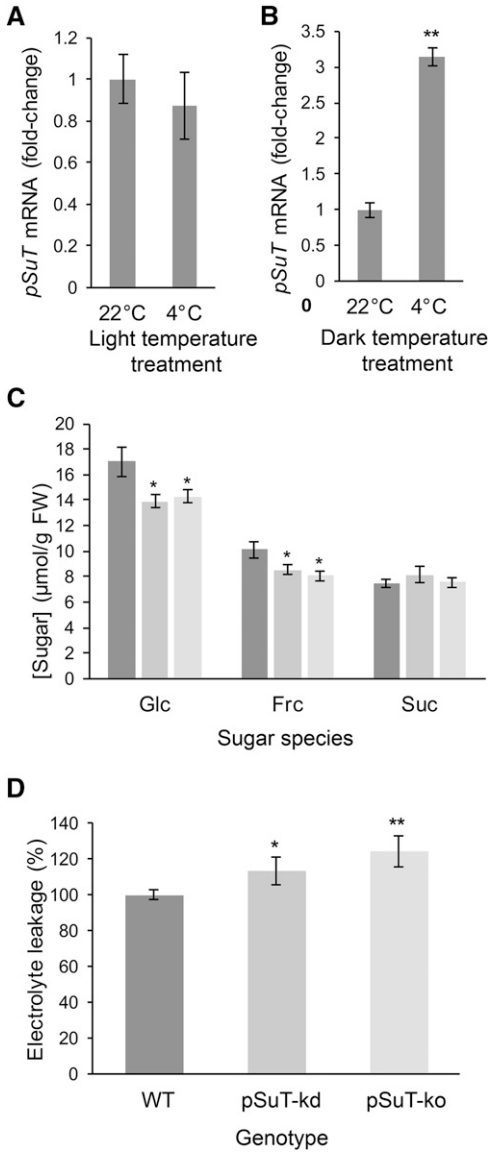

Figure 10. pSuT is required for maximal freezing tolerance. A and B, Analysis of cold-associated changes in *pSuT* transcript levels. The transcript level of plants cultivated at 22°C served as a reference (set to 1). Data were normalized to the expression of the housekeeping genes *At5g08290* and *At1g13320* and represent means of four biological replicates ± SE. Significance differences were calculated using one-factor ANOVA (**, $P \leq 0.01$). A, Analysis of *pSuT* transcript levels of wild-type plants cultivated for 4 weeks at 22°C under short-day conditions, then at 4°C for 24 h under short-day conditions. B, Analysis of *pSuT* transcript levels of wild-type plants cultivated for 4 weeks at 22°C, then at 4°C for 24 h in the dark. C, Sugar levels in 4-week-old rosette leaves of wild-type (dark gray bars), *pSUT-kd* (gray bars), and *pSuT-ko* (light gray bars) plants after exposure to cold (4°C, short-day conditions) for 24 h. Frc, Fru. Data are means from 10 plants per line ± SE. Significant differences compared with the wild type were calculated using one-tailed Student's *t* test (*, $P \leq 0.05$). D, Analysis of the electrolyte leakage from leaves of wild-type (dark gray bars), *pSuT-kd* (gray bars), and *pSuT-ko* (light gray bars) plants after 4 d of cold (4°C) acclimation. Electrolyte leakage from mutant plant leaves was normalized to leakage from wild-type leaves (set to 100%). Data represent means of at least 18 biological replicates ± SE. Significant differences compared with the wild type were calculated using one-tailed Student's *t* test (*, $P \leq 0.05$ and **, $P \leq 0.01$).

weight Fru, whereas wild-type leaves exhibited about 17 μmol g^{-1} fresh weight Glc and 10 μmol g^{-1} fresh weight Fru. The lesser contents of Glc and Fru suggest that *pSuT* mutant plants trap a certain amount of cellular Suc in the plastid stroma, which thus cannot become cleaved by extraplastidic (most likely vacuolar) invertases.

The data presented here imply that altered pSuT activity affects subcellular sugar distribution and carbohydrate metabolism in the cold. Notably, a tightly controlled and adequately adapted sugar metabolism and compartmentation are prerequisites for cold acclimation and the acquisition of freezing tolerance. Via an electrolyte leakage assay, we tested the ability of mutant and wild-type plants to resist subzero temperatures. To this end, we transferred 3-week-old wild-type and *pSuT* mutant plants for 4 d into the cold (4°C) to allow for their acclimation to low temperatures. After this phase, leaf samples were cooled down to −6°C in water and, after rethawing, the release of ions from disrupted cells was quantified via electroconductivity of the supernatant. Interestingly, leaves of *pSuT-kd* and *pSuT-ko* mutants released 14% and 24%, respectively, more electrolytes than those of wild type (set to 100%; Fig. 10D). This observation indicates that not only vacuolar but also plastidic sugar transport contributes to the acquisition of freezing tolerance.

DISCUSSION

For decades, it has been well known that specific monosaccharides, disaccharides, and oligosaccharides leave and enter the chloroplast via protein-mediated transport. However, until now, only two plastidic sugar transporters, namely MEX1 and pGlcT, have been characterized at the molecular level. MEX1 exports the starch degradation product maltose (Niittylä et al., 2004; Findinier et al., 2017), and its absence in mutant plants results in the inhibition of starch degradation due to the accumulation of this sugar in the stroma. This metabolic disturbance is connected to growth retardation, which is due to the reduced nocturnal delivery of carbohydrates to the cytosol (Niittylä et al., 2004; Lu and Sharkey, 2006). By contrast, the impaired Glc transport in mutants lacking pGlcT (Weber et al., 2000) does not markedly affect plant metabolism or development (Cho et al., 2011). However, since chloroplasts contain, besides maltose and Glc, additional neutral sugars, we must assume that other sugar transporters exist in the chloroplast envelope. In this study, we characterized a previously unknown member of the MST family, which led to the identification of a third plastidic sugar transporter, now termed pSuT.

pSuT Resides in the Inner Plastid Envelope

In phylogenetic analyses of the Arabidopsis MST family, pSuT is part of a subfamily together with the two vacuolar Glc transporters VGT1 and VGT2 (Supplemental Fig. S1). However, in contrast to its vacuolar pendants, its

amino acid sequence exhibits an N-terminal extension consisting of a chloroplast transit peptide (Supplemental Fig. S2) and a membrane protein leader (Rolland et al., 2016). Such a bipartite N-terminal sequence extension was shown recently to be typical for larger membrane proteins of the inner plastid envelope (Rolland et al., 2016).

The specific characteristics of the N terminus suggest that pSuT is located in the plastid, where it resides in the innermost envelope membrane, and various experimental data supported this assumption. First, the transient expression of a pSuT-GFP fusion protein in tobacco (Rolland et al., 2016) or Arabidopsis (Fig. 1) protoplasts resulted in a green fluorescence signal surrounding the red fluorescence caused by the chlorophyll. Second, import assays with the radioactively labeled protein suggest that pSuT integrates into the inner envelope membrane of the chloroplast (Fig. 1; Supplemental Fig. S4). This is because the size of the radioactively labeled pSuT precursor decreased after import and because the truncated protein is resistant against cleavage by externally added thermolysin. Similar results have been obtained with various inner envelope membrane proteins (Knight and Gray, 1995; Neuhaus et al., 1997; Weber et al., 2000). The decrease of the apparent molecular mass and the thermolysin resistance are generally indicative for removal of the chloroplast transit peptide and a subsequent import of the mature protein in the inner envelope membrane. Third, missing pSuT activity results in the alteration of plastidic and cytosolic sugar levels (Fig. 6) and, thus, leads to impaired sugar passage across the chloroplast envelope membrane.

Analysis of hybrid constructs revealed that the N terminus of pSuT contains all information required for successful plastid targeting, since it is sufficient to direct cyanobacterial bicarbonate transporters (Rolland et al., 2016) as well as the vacuolar sugar transporters VGT1 and SUC4 (Fig. 1; Supplemental Fig. S4) to the chloroplast. Moreover, exchange of the pSuT N terminus with that of VGT1 led to the redirection of pSuT from the chloroplast to the tonoplast (Fig. 1). These results demonstrate that the respective N termini, and thus comparatively small amino acid sequences, determine whether the corresponding protein enters either the so-called posttranslational import pathway typical for chloroplasts or the cotranslationally organized import into the endoplasmic reticulum required for targeting into the vacuolar membrane. In this context, however, we have to keep in mind that most members of the MST family are located in the plasma membrane or tonoplast and that plastidic MST-type sugar transporters clearly represent the exception (Pommerrenig et al., 2018). Therefore, it is tempting to speculate that pSuT evolved from a vacuolar or plasma membrane-located ancestor of the VGT subfamily. Consequently, pSuT might contain internal (relict) sequence information for endoplasmic reticulum entry and further targeting via the secretory pathway that is overruled by the chloroplast transit peptide and the membrane protein leader sequence in planta. In fact, pSuT can enter the vacuole even without any N-terminal domain, at least when expressed in yeast (Supplemental Fig. S5).

pSuT Transports Glc and Suc Possibly in Antiport with Protons

The affiliation of pSuT with the MSTs, its basic structure, and particularly the typical sugar-binding motifs in its amino acid sequence (Supplemental Fig. S2) classify this protein as a sugar transporter. Initial analyses led to the assumption that pSuT might catalyze the transport of Xyl (with a remarkably low affinity; Hector et al., 2008), which, however, was disproven by two independent experimental approaches (Runquist et al., 2010). Moreover, the transport of Xyl into or out of the chloroplast is highly unlikely, since these organelles have never been linked to the metabolism of Xyl, a very-low-abundance sugar in plant cells. In contrast, the observation that MST members with identical biochemical properties usually phylogenetically cluster together and form functional subfamilies (Supplemental Fig. S1; Pommerrenig et al., 2018) suggests that pSuT, just like its closest homolog VGT1, might rather operate as an H^+/Glc antiporter.

Both qualitative and quantitative growth analyses of yeast cells expressing a tonoplast-located pSuT variant (ΔTP-pSuT) indicate that the recombinant protein may catalyze Glc uptake into the vacuole (Fig. 2) and that the corresponding transport is driven by the proton gradient across the tonoplast. These conclusions are based on the observations that, in the presence of 2-dGlc, yeast cells propagated efficiently only when expressing ΔTP-pSuT, whereas the control strain showed highly retarded growth (Fig. 2). The ability to tolerate the toxic sugar derivative requires its efficient sequestration into the vacuole, which attenuates the detrimental effects of 2-dGlc on metabolism and, thus, on growth (Fig. 2). Therefore, the transport of 2-dGlc against a concentration gradient is likely to occur. In fact, yeast cells expressing the recombinant pSuT version accumulate the fluorescing Glc analog 2-NBDG in their vacuoles, whereas 2-NBDG remained in the cytosol in control cells (Fig. 3). The substantial concentration of 2-NBDG in yeast vacuoles suggests that pSuT mediates Glc uptake and that this transport is driven by the antiport of protons.

Esculin has been used frequently as a fluorescent probe to identify Suc transport capacities of selected plant sugar transporters (Sivitz et al., 2007; Gora et al., 2012; Nieberl et al., 2017; Rottmann et al., 2018a). Yeast cells expressing the Suc loader AtSUC2 gained the capacity to take up esculin from the medium (Fig. 3), but solely the additional presence of the vacuolar pSuT version led to substantial esculin relocation from the cytosol to the vacuole (Fig. 3). Thus, the observed vacuolar accumulation of esculin against a concentration gradient strongly suggests that Suc represents an additional substrate of pSuT and that this sugar also is transported in a proton/sugar antiport mode.

At first glance, the Suc transport capacity of pSuT is surprising, since the structures and the molar masses of Glc and Suc differ markedly and because members of the MST family generally are quite specific for monosaccharides (Slewinski, 2011). However, there are

further MST members showing a broad substrate spectrum, namely the tonoplast-located sugar transporters TST. Electrophysiological studies revealed that the Arabidopsis transporter TST1 and the sugar beet (*Beta vulgaris*) homolog BvTST1 transport both Glc and Suc with similar efficiency, as indicated by the fact that comparable proton flux caused currents across the tonoplast (Schulz et al., 2011; Jung et al., 2015). Moreover, BvTST2.1 even prefers Suc specifically when compared with its Glc transport activity (Jung et al., 2015). Therefore, at least a few MST members possess the capacity for Suc transport.

Toward the in Vivo Function of pSuT

The transport analyses in the heterologous yeast expression system provide the first indirect hints that pSuT transports Glc and Suc in antiport with protons. However, the question arises whether, in planta, pSuT also mediates a proton-driven transport of Suc and Glc across the inner plastid envelope.

Independent experimental data led to the assumption that pSuT exports sugars out of the plastid. First, externally added monosaccharides and disaccharides were shown to cause massive reduction in *pSuT* transcript abundance (Fig. 4J). Generally, sugar feeding results in the up- and down-regulation of vacuolar sugar importer and exporter genes, respectively (Wormit et al., 2006; Poschet et al., 2011; Chardon et al., 2013; Klemens et al., 2014; Jung et al., 2015). This differential gene expression guarantees cytosolic sugar homeostasis by the sequestration of excess sugars into the vacuole. Similarly, the marked sugar repression of *pSuT* expression indicates that pSuT acts as a sugar exporter, providing sugars to the cytosol when needed. Moreover, NAF analyses not only supported the assumption that pSuT is a sugar exporter but also suggest that Suc represents the preferred in vivo substrate. Leaves of the *pSuT-ko* mutants show altered subcellular distribution of Suc but not of Glc or Fru when compared with that of wild-type leaves (Fig. 6). More precisely, the absence of pSuT resulted in higher plastidic and lower cytosolic Suc levels. This observation already implies that pSuT facilitates Suc export out of the chloroplast. Moreover, chloroplasts from various species apparently contain higher levels of Suc than Glc (Fig. 6; Heber, 1957; Fürtauer et al., 2016); thus, Suc might outcompete Glc during binding and export. However, we have to keep in mind that the elevated Suc level in the chloroplasts of the mutant plants might alternatively result from a reduced export of hexoses in conjunction with altered plastidic invertase activity.

Transport studies with the recombinant protein suggest that pSuT catalyzes the transport of sugars in antiport with protons; therefore, it is tempting to speculate that this also applies to the in vivo situation. In fact, the cytosolic pH of mesophyll cells is supposed to be more acidic (pH 7.2; Smith, 1979) than that of the stroma (pH 8; Smith, 1979). Thus, the resulting proton gradient could allow for sugar export via pSuT (Werdan et al., 1975).

The proposed Suc export capacity of pSuT and the resulting decrease in cytosolic Suc also can explain the phenotypic peculiarities of the *pSuT* mutant plants. Interestingly, physiological analyses identified cytosolic Suc as a key regulator in flowering onset (Bolouri Moghaddam and Van den Ende, 2013), apical dominance, and bud outgrowth (Mason et al., 2014). The *pSuT* mutant lines are delayed in bolting and exhibit a reduced number of inflorescence branches (Figs. 7 and 9); in this, they closely resemble mutant plants with increased sucrolytic activity in the cytosol (Heyer et al., 2004). By contrast, the increased cytosolic Suc biosynthesis capacity results in enhanced shoot branching (Otori et al., 2017). The delay in flowering initiation concurs with significantly lower levels of *FT* mRNA levels in the *pSuT* plants (Fig. 7B). The latter regulator of transcription factors is required for flowering induction (Wickland and Hanzawa, 2015), and the expression of its gene is regulated by the cytosolic Suc concentration (Wingler et al., 2012; Wahl et al., 2013). Until now, however, it was unclear whether Suc acts as a signal in flowering induction and shoot branching directly or indirectly via trehalose-6-phosphate signaling (Wingler, 2018). Moreover, we have to keep in mind that, besides its regulatory function, Suc can act simply as a carbon source during plant growth. Thus, a lower availability of phloem-mobile Suc might impair shoot and silique development, as observed in the *pSuT* mutant lines (Figs. 7 and 8).

Cold acclimation involves substantial changes in sugar metabolism and compartmentation (Rosa et al., 2009; Nägele and Heyer, 2013; Tarkowski and Van den Ende, 2015). When exposed to cold temperatures, plants accumulate high amounts of soluble sugars, including Suc (Sasaki et al., 1996). The availability of Suc in the cytosol is apparently essential for the acquisition of maximal freezing tolerance (Strand et al., 2003), since its cleavage by invertases delivers monosaccharides that may induce the expression acclimation-relevant genes (Klotke et al., 2004; Rekarte-Cowie et al., 2008). Interestingly, in the first days of cold exposure, the extremely cold-tolerant Arabidopsis accessions Rschew (Russia) and Tenela (Scandinavia) exhibit very high cytosolic Suc concentrations, supposedly to serve as a transient cryoprotectant (Nägele and Heyer, 2013). Moreover, winter leaves of the markedly frost-hardy bugle-herb (*Ajuga reptans*) show a different compartmentation of Suc than summer leaves, implying that frost hardiness involves the relocation of Suc from the stroma and the cytosol to the vacuole (Findling et al., 2015).

Alterations in sugar compartmentation suggest that vacuolar and plastidic sugar transport processes are modified when the plant perceives the cold signal. Several studies suggest that the activity or expression of vacuolar sugar transporters is regulated differently in response to cold and that changes in their abundance may influence freezing tolerance (Wormit et al., 2006; Klemens et al., 2013; Guo et al., 2014). For almost 10 years, it has been known that raffinose is actively imported into the chloroplast (Schneider and Keller, 2009), where it acts as a cryoprotectant of the

thylakoids, but the corresponding transporter remains to be identified. However, for the following reasons, we propose that pSuT plays a role in cold acclimation. First, the expression of *pSuT* is apparently up-regulated by cold temperatures (Fig. 10B). Because high sugar levels almost completely inhibit *pSuT* transcription under ambient conditions (Fig. 4J), this regulation guarantees efficient *pSuT* expression, even when sugars accumulate in response to cold temperatures (Fig. 10A). Second, after cold exposure, *pSuT* mutants accumulate less Glc and Fru than the wild type (Fig. 10C). Third, *pSuT* mutant plants are more sensitive to freezing than wild-type plants (Fig. 9D). The decrease in monosaccharide accumulation and the lower freezing tolerance apparently result from impaired plastidic sugar transport and, most likely, from limited Suc delivery to the cytosol. We propose that the chloroplast might act as a Suc reservoir and that pSuT allows for the fast delivery of Suc in response to cold temperatures. The exported Suc can interact directly with the organellar membranes, fuel raffinose production in the cytosol, or be cleaved to Glc and Fru by cytosolic or vacuolar invertases. Due to the impaired pSuT activity, Suc is trapped in the stroma of the mutant plants (Fig. 6) and, thus, cannot enter cold-dependent carbohydrate metabolism in the cytosol and vacuole. The reduced cytosolic and vacuolar Suc availability leads to lower Fru and Glc production via invertases (Fig. 10C). The accumulation of monosaccharides (Poschet et al., 2011; Klemens et al., 2014) and the relocation of Suc from the plastid to the cytosol and finally to the vacuole (Nägele and Heyer, 2013; Findling et al., 2015), however, are critical factors in the acquisition of freezing tolerance.

The presence of Suc and Suc-dependent enzymes in the stroma as well as the proposed Suc export function of pSuT imply that Suc has to enter the chloroplast. Currently, we can only speculate on the molecular nature of a plastidic Suc importer. Until now, only two further plastidic sugar transporters, namely MEX1 and pGlcT (Weber et al., 2000; Niittylä et al., 2004), have been identified. Detailed analyses of the physiological properties of *mex1* mutants led to the speculation that this carrier might transport, besides maltose, other substrates as well (Ryoo et al., 2013; Findinier et al., 2017). Several plasma membrane-located Suc transporters were shown to transport maltose in addition to Suc (Meyer et al., 2000; Barth et al., 2003; Sivitz et al., 2007); similarly, MEX1 might transport both maltose and Suc. However, in contrast to maltose, Suc would have to be imported by MEX1. Alternatively, pGlcT could exhibit a thus far hidden affinity for Suc (Weber et al., 2000; Findinier et al., 2017), or another chloroplast-located transporter that awaits molecular characterization acts as a Suc loader (e.g. the proposed raffinose importer may catalyze Suc uptake; Schneider and Keller, 2009).

CONCLUSION

Sugars are an excellent source of cellular energy provision, are precursors in various anabolic processes, represent signal molecules governing gene expression and developmental processes, and are essential components in stress tolerance. Here, we characterized the plastidic sugar exporter pSuT, which represents a novel element required for the control of flowering onset, the determination of plant organ architecture, and the acquisition of maximal freezing tolerance.

MATERIALS AND METHODS

Plant Material and Growth Conditions

Arabidopsis (*Arabidopsis thaliana*) ecotype Columbia-0 plants were cultivated in a growth chamber on soil (ED-73; Patzer) under 22°C and 120 μmol $m^{-2} s^{-1}$ for 10 h per day. Analyses of leaf material were performed after 4 weeks of cultivation. For the investigation of the flowering phenotype, plants were transferred to LD conditions (22°C and 200 μmol $m^{-2} s^{-1}$ for 16 h per day) after cultivation for 4 weeks under standard conditions.

Subcellular Localization

For subcellular localization, pSuT- and VGT1-GFP fusion constructs were generated. Coding sequences were amplified with specific primers AtpSuT_fwd/AtpSuT_rev and AtVGT1_fwd/AtVGT1_rev, respectively, and ligated into *Sma*I–digested pBluescript II KS(+) (for primer information, see Supplemental Table S1). The resulting constructs served as templates for amplification with either AtpSuT_gw_fwd/AtpSuT_gw_rev or AtVGT1_gw_fwd/AtVGT1_gw_rev primers, containing attB1 and attB2 sites required for recombination of the PCR product with $pDONR_{zeo}$ (Invitrogen) via its attP sites (Gateway BP reaction, generation of the entry clone). The expression vector was generated by recombination between the attL sites of the entry clone and the attR sites of the destination vector p*7FWG2.0 (Karimi et al., 2002; Gateway LR reaction). The transformation of Arabidopsis mesophyll protoplasts was performed as described by Yoo et al. (2007). For localization of the $N\text{-term}_{pSuT}$VGT1-fusion construct, an overlapping PCR was performed. The N-terminal sequence of pSuT was amplified with pSuT_fora and pSuT/VGT1_reva primers. The VGT1 coding sequence (beginning from the start of the conserved region as shown in Supplemental Fig. S2) was amplified with pSuT/VGT1_forb and VGT1_revb primers. Both PCR products were used as templates for overlapping PCR with pSuT_fora and VGT1_revb. Similarly, the $N\text{-term}_{vgt1}$pSuT-fusion construct was generated with VGT1_for and VGT1/pSuT_rev primers for amplification of the N terminus of VGT1 and with VGT1/pSuT_for and pSuT_rev-s for amplification of the pSuT coding sequences. For overlapping PCR, the VGT1_for and pSuT_rev-s primers were used. Gateway cloning was conducted as outlined above with construct-specific primers (pSuT_Koz_gw_for/VGT1_gw_rev-s and VGT1_gw_fwd/AtpSuT_gw_rev-s).

Gene Expression Analyses

Expression analyses were performed by RT-qPCR. RNA was extracted from frozen leaves or leaf discs with the NucleoSpin RNA Plant Kit (Macherey-Nagel) according to the manufacturer's advice. RNA was transcribed into cDNA with the qScript cDNA Synthesis Kit (Quantabio). According to the experimental conditions, *At4g26410*, *AtPP2A-A3*, *AtUBQ10*, *AtUBC9*, *AtSAND*, *AtTUB2*, and *AtYLS8* served as reference genes for transcript normalization.

Identification of pSuT T-DNA Insertion Lines

The Arabidopsis T-DNA insertion lines *pSuT-ko* (Salk_021796) and *pSuT-kd* (Sail_335_F05) were provided by the Nottingham Arabidopsis Stock Centre (http://arabidopsis.info/). Verification of homozygosity of the T-DNA insertion lines was performed by PCR. LP_ko, RP_ko, and T-DNA-specific Lbb1.3 primers were used for Salk_021796, and LP_kd, RP_kd, and T-DNA-specific LB1 primers were used for Sail_335_F05. The *pSuT* transcript level was verified via RT-qPCR by the use of RT-F and RT-R primers, and the *At5g59240* transcript level was verified using AtRPS8E_fwd and AtRPS8E_rev primers.

Metabolite Extraction and Quantification

For sugar isolation, leaves were harvested, frozen in liquid nitrogen, and stored at −80°C until use. In the first step of extraction, 500 μL of water was

added to 50 mg of ground plant material, mixed thoroughly, and heated to 95°C for 15 min. After centrifugation, the supernatant was used for metabolite quantification. For the isolation of starch, the pellet was washed twice with 80% (w/v) ethanol and autoclaved in 50 mM sodium acetate, pH 4.7. Subsequently, the samples were digested with 5 units of α-amylase and β-amyloglucosidase for 4 h and spun down, and the supernatant was used for Glc quantification. Metabolite quantification was performed using an NADP-coupled enzymatic test (Stitt et al., 1989).

Electrolyte Leakage Analyses

The electrical conductivity of frozen leaves of the wild type, *pSut-kd*, and *pSuT-ko* was determined based on Ristic and Ashworth (1993) as follows. Three-week-old plants were acclimated to 4°C for 4 d. Mature leaves were added to glass tubes with 2 mL of deionized water, separately. Test tubes were incubated at 0°C for 1 h, and the temperature was decreased to −6°C (in steps of 1°C per 30 min). Freezing of the water surrounding the leaves was introduced by the addition of ice chips at −1°C. Samples were thawed slowly overnight in a cold room (4°C), and the tubes were shaken gently at 4°C as the complete absence of ice crystals was ensured. After 24 h, 3 mL of deionized water was added, and the samples were shaken for 1 h at room temperature. Electrolyte leakage was measured at room temperature using a WTW LF521 conductivity meter (Wissenschaftlich-Technische Werkstätten). To determine the total electrical conductivity (reference value), the samples were boiled for 2 h. Data were normalized to that in the wild type.

NAF

The sugar compartmentation of wild-type and *pSuT-ko* leaf material was determined by NAF of 4-week-old plants. The experimental procedure proceeded as described by Krüger et al. (2011) and Arrivault et al. (2014). Nitrate was used as a vacuolar marker, UGPase activity as a cytosolic marker, and chlorophyll as a plastidic marker. For sugar quantification, an NADP-coupled enzymatic test was performed (Stitt et al., 1989). Subcellular metabolite distribution was calculated using the BestFit algorithm according to Riens et al. (1991).

Protein Import Assay

The *pSuT* gene was amplified from cDNA with gene-specific primers (*At*pSuT_fwd and *At*pSuT_rev), ligated into *Sma*I-digested pBluescript II KS(+), and served as a template to amplify the gene with T7 and pSuT-6TM *Sal*I primers. The PCR product was digested with *Eco*RI/*Sal*I and ligated into *Eco*RI/*Sal*I-digested pSP65 vector. Transcription was performed in a final volume of 50 μL in the presence of SP6 RNA polymerase. The mixture included polymerase buffer, 100 units of RNase inhibitor, 10 mM DTT, 25 μM BSA, 2.5 mM m7 GpppG, 2.5 mM each ATP, CTP, and UTP, and 3 μg of linearized plasmid. After 30 min of incubation at 37°C, 1.2 mM GTP was added, and RNA synthesis was continued for 2 h at 37°C. The synthesized mRNA was used for translation in a final volume of 100 μL. Wheat germ extract (Promega) was supplemented with RNase inhibitor, amino acids without Met, and [^{35}S]Met/Cys (145 μCi), and translation was conducted for 45 min at 30°C. Chloroplasts were isolated from 8- to 10-d-old pea (*Pisum sativum*) plants according to Waegemann and Soll (1991). The concentration of chlorophyll was determined as described (Arnon, 1949). A standard import reaction contained chloroplasts equivalent to 20 μg of chlorophyll in 100 μL of import buffer (330 mM sorbitol, 50 mM HEPES/KOH, pH 7.6, 3 mM $MgSO_4$, 10 mM Met, 10 mM Cys, 20 mM K-gluconate, 10 mM $NaHCO_3$, 2% [w/v] BSA, and 3 mM ATP) and 1% to 8% ^{35}S-labeled precursor protein. The import reaction was conducted for 15 min at 25°C unless indicated otherwise. Chloroplasts were reisolated by centrifugation through a 40% Percoll cushion and washed twice in wash medium (330 mM sorbitol, 50 mM HEPES/KOH, pH 7.6, and 0.5 mM $CaCl_2$). Where indicated, chloroplasts were treated with 100 μg mL^{-1} thermolysin after import for 20 min on ice. Imported proteins were separated by SDS-PAGE and analyzed with a phosphor imager (FLA3000; Fuji).

Cloning of pSuT-GUS and Histochemical GUS Staining

For the generation of *pSuT* promoter-GUS plants, a 1,779-bp fragment upstream of the pSuT coding sequence was amplified with pSuTpro_fwd and pSuTpro_rev primers and cloned into *Sma*I-digested pBluescript II KS(+). This was used as a template for Gateway cloning with pSuTpro_GW_fwd and pSuTpro_GW_rev primers, using the specific destination vector p*GWFS7 (Karimi et al., 2002). After transformation of *Agrobacterium tumefaciens* (GV3101), Arabidopsis *pSuT* promoter-GUS plants were generated using the floral dip method as described by Clough and Bent (1998). Histochemical GUS staining was conducted as described by An et al. (1996).

Heterologous Expression of ΔTP-pSuT-GFP in Yeast

The *pSuT* gene lacking its N-terminal chloroplast transit peptide sequence (*ΔTP-pSuT*) was amplified with AtpSuTgwFWD-TP31 and AtpSuT_gw_rev-s primers and used for recombination into pDONRzeo and the shuttle vector pGWFDR196 (Li et al., 2008) to express *ΔTP-pSuT* with C-terminal GFP. The baker's yeast (*Saccharomyces cerevisiae*) strain W303 (*MATa/MATα {leu2-3,112 trp1-1 can1-100 ura3-1 ade2-1 his3-11,15} [phi$^+$]*) was used for all transformations and experiments. Yeast cell transformation was carried out according to Gietz and Schiestl (2007). The vacuolar localization of ΔTP-pSuT-GFP was analyzed by fluorescence microscopy. Yeast droplet tests were conducted by using SC medium supplemented with 1% (w/v) Glc and 1% (w/v) Glc + 0.2% (w/v) 2-dGlc on solid medium. Yeast culture was grown for 18 h at 30°C until logarithmic phase (OD_{600} = 1) and was diluted subsequently. For growth kinetics, yeast was cultivated in liquid SC medium for 18 h at 30°C until logarithmic phase, diluted, and added to SC medium with 2% (w/v) Glc and 2% (w/v) Glc + 0.2% (w/v) 2-dGlc, with a initial OD_{600} of 0.005. The growth curve was determined every 1 min for 60 h by measuring the OD_{600} using a 96-well UV-visible spectrophotometer (Tecan Infinite 200; Tecan Group).

2-NBDG Assay in Yeast

For yeast strains expressing ΔTP-pSuT without the GFP signal, pDONOR-pSUT-TP31 was recombined with the plasmid pDRF1-GW (Loqué et al., 2007) via the attL and attR sites (Gateway LR reaction). pDRf1-GW was a gift from Woei-Jiun Guo from Taiwan University. The empty vector was generated by cutting out the Gateway cassette in pDRF1-GW using *Xho*I. Yeast was cultivated in SC medium containing 2% (w/v) Glc and the suitable amino acid until logarithmic phase. The 2-NBDG assay was performed as described by Zhang et al. (2015) with the following modifications: the culture was treated with 2-NBDG (Life Technologies) at a final concentration of 400 μM, and the cells were incubated at 30°C with shaking at 450 rpm for 5 h.

Esculin Assay in Yeast

Yeast (W303) harboring pDRF1-pSUT-SP31 and the empty vector was transformed with pSUC2-Leu to verify the uptake of esculin into the yeast cytosol. Arabidopsis SUC2 cDNA was amplified from RNA from Arabidopsis leaves using the primers AtSUC2c+1f and AtSUC2c+1539r. The primers introduced *Eco*RI cloning sites at both cDNA ends and inserted a 15-bp sequence (5′-AAGCTTGTAAAAGAA-3′) upstream of the start codon known to improve the expression of foreign proteins in yeast (Pommerrenig et al., 2011). Sequenced PCR products were cloned into the yeast/*Escherichia coli* shuttle vector NEV-E/Leu, allowing the use of Leu as an auxotrophy marker for successfully transformed yeast cells (Sauer and Stolz, 1994). The resulting plasmid pSUC2-Leu was used for subsequent cotransformation of yeast cells with pDRF1-pSUT-SP31 and with the empty pDRF1-vector. Yeast cells were treated as for the 2-NBDG assay but with incubation with 1 mM esculin for 13 h.

Microscopy

For fluorescence microscopy, a Leica TCS SP5II confocal laser scanning microscope was used, and photographs were taken using the Leica HCX PL APO 63·/1.20 w mot CORR CS objective with a Vis Argon Laser with the settings 494 to 551 nm suitable for GFP and 2-NBDG and 465 to 550 nm suitable for esculin. For the imaging of GUS staining, a Leica MZ10F modular stereomicroscope was used, and photographs were taken using a Leica DFC420C digital microscope camera.

Accession Numbers

Sequence data from this article can be found in the GenBank/EMBL data libraries under accession numbers BT015354.1 (*pSUT*, *At5g59250*), BT010375.1

(*VGT1*, *At3g03090*), AY114066.1 (*VI1*, *AT1G62660*), and AY065378.1 (*FT*, *At1g65480*).

Supplemental Data

The following supplemental materials are available.

Supplemental Figure S1. Phylogenetic relationships of members of the MST family from Arabidopsis.

Supplemental Figure S2. Alignment of VGT1, VGT2, and pSuT from Arabidopsis.

Supplemental Figure S3. Import of pSuT into isolated chloroplasts.

Supplemental Figure S4. Localization of N-termpSuTSUC4 and VGT1 in Arabidopsis protoplasts.

Supplemental Figure S5. Truncation of the chloroplast transit peptide causes vacuolar targeting of pSuT in yeast.

Supplemental Figure S6. Isolation of two independent T-DNA insertion lines for *pSuT*.

Supplemental Figure S7. Relative transcript level of the putative *VI1*.

Supplemental Table S1. List of primers used in this study.

ACKNOWLEDGMENTS

We thank Ruth Wartenberg and Maximilian Rother (both Plant Physiology, University of Kaiserslautern) for excellent technical assistance and analysis of promoter-pSUT-GUS plants.

Received August 27, 2018; accepted November 13, 2018; published November 27, 2018.

LITERATURE CITED

Alberdi M, Corcuera LJ (1991) Cold acclimation in plants. Phytochemistry **30:** 3177–3184

Aluri S, Büttner M (2007) Identification and functional expression of the *Arabidopsis thaliana* vacuolar glucose transporter 1 and its role in seed germination and flowering. Proc Natl Acad Sci USA **104:** 2537–2542

An YQ, Huang S, McDowell JM, McKinney EC, Meagher RB (1996) Conserved expression of the Arabidopsis ACT1 and ACT3 actin subclass in organ primordia and mature pollen. Plant Cell **8:** 15–30

Arnon DI (1949) Copper enzymes in isolated chloroplasts: Polyphenoloxidase in *Beta vulgaris*. Plant Physiol **24:** 1–15

Arrivault S, Guenther M, Florian A, Encke B, Feil R, Vosloh D, Lunn JE, Sulpice R, Fernie AR, Stitt M, et al (2014) Dissecting the subcellular compartmentation of proteins and metabolites in Arabidopsis leaves using non-aqueous fractionation. Mol Cell Proteomics **13:** 2246–2259

Barbier FF, Lunn JE, Beveridge CA (2015) Ready, steady, go! A sugar hit starts the race to shoot branching. Curr Opin Plant Biol **25:** 39–45

Barth I, Meyer S, Sauer N (2003) PmSUC3: Characterization of a SUT2/SUC3-type sucrose transporter from *Plantago major*. Plant Cell **15:** 1375–1385

Bisson LF, Coons DM, Kruckeberg AL, Lewis DA (1993) Yeast sugar transporters. Crit Rev Biochem Mol Biol **28:** 259–308

Bolouri Moghaddam MR, Van den Ende W (2013) Sugars, the clock and transition to flowering. Front Plant Sci **4:** 22

Bush DR (1999) Sugar transporters in plant biology. Curr Opin Plant Biol **2:** 187–191

Büttner M (2007) The monosaccharide transporter(-like) gene family in Arabidopsis. FEBS Lett **581:** 2318–2324

Chardon F, Bedu M, Calenge F, Klemens PA, Spinner L, Clement G, Chietera G, Léran S, Ferrand M, Lacombe B, et al (2013) Leaf fructose content is controlled by the vacuolar transporter SWEET17 in Arabidopsis. Curr Biol **23:** 697–702

Chen HY, Huh JH, Yu YC, Ho LH, Chen LQ, Tholl D, Frommer WB, Guo WJ (2015a) The Arabidopsis vacuolar sugar transporter SWEET2 limits carbon sequestration from roots and restricts *Pythium* infection. Plant J **83:** 1046–1058

Chen LQ, Cheung LS, Feng L, Tanner W, Frommer WB (2015b) Transport of sugars. Annu Rev Biochem **84:** 865–894

Cho MH, Lim H, Shin DH, Jeon JS, Bhoo SH, Park YI, Hahn TR (2011) Role of the plastidic glucose translocator in the export of starch degradation products from the chloroplasts in Arabidopsis thaliana. New Phytol **190:** 101–112

Clough SJ, Bent AF (1998) Floral dip: A simplified method for Agrobacterium-mediated transformation of Arabidopsis thaliana. Plant J **16:** 735–743

Corbesier L, Lejeune P, Bernier G (1998) The role of carbohydrates in the induction of flowering in *Arabidopsis thaliana*: Comparison between the wild type and a starchless mutant. Planta **206:** 131–137

Corbesier L, Vincent C, Jang S, Fornara F, Fan Q, Searle I, Giakountis A, Farrona S, Gissot L, Turnbull C, et al (2007) FT protein movement contributes to long-distance signaling in floral induction of Arabidopsis. Science **316:** 1030–1033

Findinier J, Tunçay H, Schulz-Raffelt M, Deschamps P, Spriet C, Lacroix JM, Duchêne T, Szydlowski N, Li-Beisson Y, Peltier G, et al (2017) The Chlamydomonas mex1 mutant shows impaired starch mobilization without maltose accumulation. J Exp Bot **68:** 5177–5189

Findling S, Zanger K, Krueger S, Lohaus G (2015) Subcellular distribution of raffinose oligosaccharides and other metabolites in summer and winter leaves of *Ajuga reptans* (Lamiaceae). Planta **241:** 229–241

Fürtauer L, Weckwerth W, Nägele T (2016) A benchtop fractionation procedure for subcellular analysis of the plant metabolome. Front Plant Sci **7:** 1912

Gietz RD, Schiestl RH (2007) Quick and easy yeast transformation using the LiAc/SS carrier DNA/PEG method. Nat Protoc **2:** 35–37

Gora PJ, Reinders A, Ward JM (2012) A novel fluorescent assay for sucrose transporters. Plant Methods **8:** 13

Guo WJ, Nagy R, Chen HY, Pfrunder S, Yu YC, Santelia D, Frommer WB, Martinoia E (2014) SWEET17, a facilitative transporter, mediates fructose transport across the tonoplast of Arabidopsis roots and leaves. Plant Physiol **164:** 777–789

Hanson J, Smeekens S (2009) Sugar perception and signaling: An update. Curr Opin Plant Biol **12:** 562–567

Heber U (1957) Zur Frage der Lokalisation von löslichen Zuckern in der Pflanzenzelle. Ber Dtsch Bot Ges **70:** 371–382

Hector RE, Qureshi N, Hughes SR, Cotta MA (2008) Expression of a heterologous xylose transporter in a *Saccharomyces cerevisiae* strain engineered to utilize xylose improves aerobic xylose consumption. Appl Microbiol Biotechnol **80:** 675–684

Hedrich R, Sauer N, Neuhaus HE (2015) Sugar transport across the plant vacuolar membrane: Nature and regulation of carrier proteins. Curr Opin Plant Biol **25:** 63–70

Henderson PJF (1991) Sugar transport proteins. Curr Opin Struct Biol **1:** 590–601

Heyer AG, Raap M, Schroeer B, Marty B, Willmitzer L (2004) Cell wall invertase expression at the apical meristem alters floral, architectural, and reproductive traits in *Arabidopsis thaliana*. Plant J **39:** 161–169

Hoekstra FA, Golovina EA, Buitink J (2001) Mechanisms of plant desiccation tolerance. Trends Plant Sci **6:** 431–438

Johnson DA, Thomas MA (2007) The monosaccharide transporter gene family in Arabidopsis and rice: A history of duplications, adaptive evolution, and functional divergence. Mol Biol Evol **24:** 2412–2423

Julius BT, Leach KA, Tran TM, Mertz RA, Braun DM (2017) Sugar transporters in plants: New insights and discoveries. Plant Cell Physiol **58:** 1442–1460

Jung B, Ludewig F, Schulz A, Meißner G, Wöstefeld N, Flügge UI, Pommerrenig B, Wirsching P, Sauer N, Koch W, et al (2015) Identification of the transporter responsible for sucrose accumulation in sugar beet taproots. Nat Plants **1:** 14001

Karimi M, Inzé D, Depicker A (2002) GATEWAY vectors for Agrobacterium-mediated plant transformation. Trends Plant Sci **7:** 193–195

Klemens PA, Patzke K, Deitmer J, Spinner L, Le Hir R, Bellini C, Bedu M, Chardon F, Krapp A, Neuhaus HE (2013) Overexpression of the vacuolar sugar carrier AtSWEET16 modifies germination, growth, and stress tolerance in Arabidopsis. Plant Physiol **163:** 1338–1352

Klemens PA, Patzke K, Trentmann O, Poschet G, Büttner M, Schulz A, Marten I, Hedrich R, Neuhaus HE (2014) Overexpression of a proton-coupled vacuolar glucose exporter impairs freezing tolerance and seed germination. New Phytol **202:** 188–197

Klotke J, Kopka J, Gatzke N, Heyer AG (2004) Impact of soluble sugar concentrations on the acquisition of freezing tolerance in accessions of *Arabidopsis thaliana* with contrasting cold adaptation: Evidence for a role of raffinose in cold acclimation. Plant Cell Environ **27:** 1395–1404

Knaupp M, Mishra KB, Nedbal L, Heyer AG (2011) Evidence for a role of raffinose in stabilizing photosystem II during freeze-thaw cycles. Planta **234:** 477–486

Knight JS, Gray JC (1995) The N-terminal hydrophobic region of the mature phosphate translocator is sufficient for targeting to the chloroplast inner envelope membrane. Plant Cell **7:** 1421–1432

Krüger S, Giavalisco P, Krall L, Steinhauser MC, Büssis D, Usadel B, Flügge UI, Fernie AR, Willmitzer L, Steinhauser D (2011) A topological map of the compartmentalized *Arabidopsis thaliana* leaf metabolome. PLoS ONE **6:** 17806

Le Hir R, Spinner L, Klemens PA, Chakraborti D, de Marco F, Vilaine F, Wolff N, Lemoine R, Porcheron B, Géry C, et al (2015) Disruption of the sugar transporters AtSWEET11 and AtSWEET12 affects vascular development and freezing tolerance in Arabidopsis. Mol Plant **8:** 1687–1690

Levitt J (1958) Frost, drought, and heat resistance. Protoplasma **6:** 1–78

Li X, Chanroj S, Wu Z, Romanowsky SM, Harper JF, Sze H (2008) A distinct endosomal Ca^{2+}/Mn^{2+} pump affects root growth through the secretory process. Plant Physiol **147:** 1675–1689

Loqué D, Lalonde S, Looger LL, von Wirén N, Frommer WB (2007) A cytosolic trans-activation domain essential for ammonium uptake. Nature **446:** 195–198

Lu Y, Sharkey TD (2006) The importance of maltose in transitory starch breakdown. Plant Cell Environ **29:** 353–366

Martinoia E, Maeshima M, Neuhaus HE (2007) Vacuolar transporters and their essential role in plant metabolism. J Exp Bot **58:** 83–102

Mason MG, Ross JJ, Babst BA, Wienclaw BN, Beveridge CA (2014) Sugar demand, not auxin, is the initial regulator of apical dominance. Proc Natl Acad Sci USA **111:** 6092–6097

Meyer S, Melzer M, Truernit E, Hümmer C, Besenbeck R, Stadler R, Sauer N (2000) AtSUC3, a gene encoding a new Arabidopsis sucrose transporter, is expressed in cells adjacent to the vascular tissue and in a carpel cell layer. Plant J **24:** 869–882

Nägele T, Heyer AG (2013) Approximating subcellular organisation of carbohydrate metabolism during cold acclimation in different natural accessions of *Arabidopsis thaliana*. New Phytol **198:** 777–787

Naseem M, Kunz M, Dandekar T (2017) Plant-pathogen maneuvering over apoplastic sugars. Trends Plant Sci **22:** 740–743

Neuhaus HE, Thom E, Möhlmann T, Steup M, Kampfenkel K (1997) Characterization of a novel eukaryotic ATP/ADP translocator located in the plastid envelope of *Arabidopsis thaliana* L. Plant J **11:** 73–82

Nieberl P, Ehrl C, Pommerrenig B, Graus D, Marten I, Jung B, Ludewig F, Koch W, Harms K, Flügge UI, et al (2017) Functional characterisation and cell specificity of BvSUT1, the transporter that loads sucrose into the phloem of sugar beet (*Beta vulgaris* L.) source leaves. Plant Biol (Stuttg) **19:** 315–326

Niittylä T, Messerli G, Trevisan M, Chen J, Smith AM, Zeeman SC (2004) A previously unknown maltose transporter essential for starch degradation in leaves. Science **303:** 87–89

Ohto M, Onai K, Furukawa Y, Aoki E, Araki T, Nakamura K (2001) Effects of sugar on vegetative development and floral transition in Arabidopsis. Plant Physiol **127:** 252–261

Otori K, Tamoi M, Tanabe N, Shigeoka S (2017) Enhancements in sucrose biosynthesis capacity affect shoot branching in Arabidopsis. Biosci Biotechnol Biochem **81:** 1470–1477

Pommerrenig B, Feussner K, Zierer W, Rabinovych V, Klebl F, Feussner I, Sauer N (2011) Phloem-specific expression of Yang cycle genes and identification of novel Yang cycle enzymes in Plantago and Arabidopsis. Plant Cell **23:** 1904–1919

Pommerrenig B, Ludewig F, Cvetkovic J, Trentmann O, Klemens PAW, Neuhaus HE (2018) In concert: Orchestrated changes in carbohydrate homeostasis are critical for plant abiotic stress tolerance. Plant Cell Physiol **59:** 1290–1299

Poschet G, Hannich B, Raab S, Jungkunz I, Klemens PA, Krueger S, Wic S, Neuhaus HE, Büttner M (2011) A novel Arabidopsis vacuolar glucose exporter is involved in cellular sugar homeostasis and affects the composition of seed storage compounds. Plant Physiol **157:** 1664–1676

Rekarte-Cowie I, Ebshish OS, Mohamed KS, Pearce RS (2008) Sucrose helps regulate cold acclimation of *Arabidopsis thaliana*. J Exp Bot **59:** 4205–4217

Riens B, Lohaus G, Heineke D, Heldt HW (1991) Amino acid and sucrose content determined in the cytosolic, chloroplastic, and vacuolar compartments and in the phloem sap of spinach leaves. Plant Physiol **97:** 227–233

Ristic Z, Ashworth EN (1993) Ultrastructural evidence that intracellular ice formation and possibly cavitation are the sources of freezing injury in supercooling wood tissue of *Cornus florida* L. Plant Physiol **103:** 753–761

Roldán M, Gómez-Mena C, Ruiz-García L, Salinas J, Martínez-Zapater JM (1999) Sucrose availability on the aerial part of the plant promotes morphogenesis and flowering of Arabidopsis in the dark. Plant J **20:** 581–590

Rolland V, Badger MR, Price GD (2016) Redirecting the cyanobacterial bicarbonate transporters BicA and SbtA to the chloroplast envelope: Soluble and membrane cargos need different chloroplast targeting signals in plants. Front Plant Sci **7:** 185

Rosa M, Hilal M, González JA, Prado FE (2009) Low-temperature effect on enzyme activities involved in sucrose-starch partitioning in salt-stressed and salt-acclimated cotyledons of quinoa (*Chenopodium quinoa* Willd.) seedlings. Plant Physiol Biochem **47:** 300–307

Rottmann TM, Fritz C, Lauter A, Schneider S, Fischer C, Danzberger N, Dietrich P, Sauer N, Stadler R (2018a) Protoplast-esculin assay as a new method to assay plant sucrose transporters: Characterization of AtSUC6 and AtSUC7 sucrose uptake activity in Arabidopsis Col-0 ecotype. Front Plant Sci **9:** 430

Rottmann T, Klebl F, Schneider S, Kischka D, Rüscher D, Sauer N, Stadler R (2018b) Sugar transporter STP7 specificity for l-arabinose and d-xylose contrasts with the typical hexose transporters STP8 and STP12. Plant Physiol **176:** 2330–2350

Roy A, Dement AD, Cho KH, Kim JH (2015) Assessing glucose uptake through the yeast hexose transporter 1 (Hxt1). PLoS ONE **10:** e0121985

Runquist D, Hahn-Hägerdal B, Rådström P (2010) Comparison of heterologous xylose transporters in recombinant *Saccharomyces cerevisiae*. Biotechnol Biofuels **3:** 5–9

Ryoo N, Eom JS, Kim HB, Vo BT, Lee SW, Hahn TR, Jeon JS (2013) Expression and functional analysis of rice plastidic maltose transporter, OsMEX1. J Korean Soc Appl Biol Chem **56:** 149–155

Saier MH Jr (2000) A functional-phylogenetic classification system for transmembrane solute transporters. Microbiol Mol Biol Rev **64:** 354–411

Sasaki H, Ichimura K, Oda M (1996) Changes in sugar content during cold acclimation and deacclimation of cabbage seedlings. Ann Bot **78:** 365–369

Sauer N, Stolz J (1994) SUC1 and SUC2: Two sucrose transporters from Arabidopsis thaliana. Expression and characterization in baker's yeast and identification of the histidine-tagged protein. Plant J **6:** 67–77

Schäfer G, Heber U (1977) Glucose transport into spinach chloroplasts. Plant Physiol **60:** 286–289

Schneider T, Keller F (2009) Raffinose in chloroplasts is synthesized in the cytosol and transported across the chloroplast envelope. Plant Cell Physiol **50:** 2174–2182

Schulz A, Beyhl D, Marten I, Wormit A, Neuhaus E, Poschet G, Büttner M, Schneider S, Sauer N, Hedrich R (2011) Proton-driven sucrose symport and antiport are provided by the vacuolar transporters SUC4 and TMT1/2. Plant J **68:** 129–136

Sivitz AB, Reinders A, Johnson ME, Krentz AD, Grof CP, Perroux JM, Ward JM (2007) Arabidopsis sucrose transporter AtSUC9: High-affinity transport activity, intragenic control of expression, and early flowering mutant phenotype. Plant Physiol **143:** 188–198

Slewinski TL (2011) Diverse functional roles of monosaccharide transporters and their homologs in vascular plants: A physiological perspective. Mol Plant **4:** 641–662

Smith JA (1979) Intracellular pH and its regulation. Annu Rev Plant Physiol **30:** 289–311

Stitt M, Lilley RM, Gerhardt R, Heldt HW (1989) Metabolite levels in specific cells and subcellular compartments of plant leaves. Methods Enzymol **174:** 518–552

Strand A, Hurry V, Gustafsson P, Gardeström P (1997) Development of Arabidopsis thaliana leaves at low temperatures releases the suppression of photosynthesis and photosynthetic gene expression despite the accumulation of soluble carbohydrates. Plant J **12:** 605–614

Strand A, Hurry V, Henkes S, Huner N, Gustafsson P, Gardeström P, Stitt M (1999) Acclimation of Arabidopsis leaves developing at low temperatures: Increasing cytoplasmic volume accompanies increased activities of enzymes in the Calvin cycle and in the sucrose-biosynthesis pathway. Plant Physiol **119:** 1387–1398

Strand Å, Foyer CH, Gustaffson P, Gardeström P, Hurry V (2003) Altering flux though the sucrose biosynthesis pathway in transgenic *Arabidopsis thaliana* modifies photosynthetic acclimation at low temperatures and in the development of freezing tolerance. Plant Cell Environ **26:** 523–535

Strauss G, Hauser H (1986) Stabilization of lipid bilayer vesicles by sucrose during freezing. Proc Natl Acad Sci USA **83:** 2422–2426

Sun L, Yang DL, Kong Y, Chen Y, Li XZ, Zeng LJ, Li Q, Wang ET, He ZH (2014) Sugar homeostasis mediated by cell wall invertase GRAIN INCOMPLETE FILLING 1 (GIF1) plays a role in pre-existing and induced defence in rice. Mol Plant Pathol **15:** 161–173

Tao Y, Cheung LS, Li S, Eom JS, Chen LQ, Xu Y, Perry K, Frommer WB, Feng L (2015) Structure of a eukaryotic SWEET transporter in a homotrimeric complex. Nature **527:** 259–263

Tarkowski ŁP, Van den Ende W (2015) Cold tolerance triggered by soluble sugars: A multifaceted countermeasure. Front Plant Sci **6:** 203

Waegemann K, Soll J (1991) Characterization of the protein import apparatus in isolated outer envelopes of chloroplasts. Plant J **1:** 149–158

Wahl V, Ponnu J, Schlereth A, Arrivault S, Langenecker T, Franke A, Feil R, Lunn JE, Stitt M, Schmid M (2013) Regulation of flowering by trehalose-6-phosphate signaling in *Arabidopsis thaliana*. Science **339:** 704–707

Wang CT, Nobel PS (1971) Permeability of pea chloroplasts to alcohols and aldoses as measured by reflection coefficients. Biochim Biophys Acta **241:** 200–212

Wanner LA, Junttila O (1999) Cold-induced freezing tolerance in Arabidopsis. Plant Physiol **120:** 391–400

Weber A, Servaites JC, Geiger DR, Kofler H, Hille D, Gröner F, Hebbeker U, Flügge UI (2000) Identification, purification, and molecular cloning of a putative plastidic glucose translocator. Plant Cell **12:** 787–802

Weichert N, Saalbach I, Weichert H, Kohl S, Erban A, Kopka J, Hause B, Varshney A, Sreenivasulu N, Strickert M, et al (2010) Increasing sucrose uptake capacity of wheat grains stimulates storage protein synthesis. Plant Physiol **152:** 698–710

Weiss J, Hiltbrand B (1985) Functional compartmentation of glycolytic versus oxidative metabolism in isolated rabbit heart. J Clin Invest **75:** 436–447

Werdan K, Heldt HW, Milovancev M (1975) The role of pH in the regulation of carbon fixation in the chloroplast stroma: Studies on CO_2 fixation in the light and dark. Biochim Biophys Acta **396:** 276–292

Wickland DP, Hanzawa Y (2015) The FLOWERING LOCUS T/TERMINAL FLOWER 1 gene family: Functional evolution and molecular mechanisms. Mol Plant **8:** 983–997

Wind J, Smeekens S, Hanson J (2010) Sucrose: Metabolite and signaling molecule. Phytochemistry **71:** 1610–1614

Wingenter K, Schulz A, Wormit A, Wic S, Trentmann O, Hoermiller II, Heyer AG, Marten I, Hedrich R, Neuhaus HE (2010) Increased activity of the vacuolar monosaccharide transporter TMT1 alters cellular sugar partitioning, sugar signaling, and seed yield in Arabidopsis. Plant Physiol **154:** 665–677

Wingler A (2018) Transitioning to the next phase: The role of sugar signaling throughout the plant life cycle. Plant Physiol **176:** 1075–1084

Wingler A, Delatte TL, O'Hara LE, Primavesi LF, Jhurreea D, Paul MJ, Schluepmann H (2012) Trehalose 6-phosphate is required for the onset of leaf senescence associated with high carbon availability. Plant Physiol **158:** 1241–1251

Wormit A, Trentmann O, Feifer I, Lohr C, Tjaden J, Meyer S, Schmidt U, Martinoia E, Neuhaus HE (2006) Molecular identification and physiological characterization of a novel monosaccharide transporter from Arabidopsis involved in vacuolar sugar transport. Plant Cell **18:** 3476–3490

Yoo SD, Cho YH, Sheen J (2007) Arabidopsis mesophyll protoplasts: A versatile cell system for transient gene expression analysis. Nat Protoc **2:** 1565–1572

Zhang W, Cao Y, Gong J, Bao X, Chen G, Liu W (2015) Identification of residues important for substrate uptake in a glucose transporter from the filamentous fungus *Trichoderma reesei*. Sci Rep **5:** 13829